



Suez Canal University
Faculty of Engineering
Electrical Engineering Department
Communication and Electronics Major



Find-Wi: WiFi sensing-based applications

By

El-Sayed Mohammed El-Sayed

Abd El-Rahman Sameh Ibrahim

Ahmad Abd El-Gwad Kamal

Merna Hamdy Ahmad

Mostafa Mahmoud El-Sayed

Abd El-Rahman Mohammed Fiala

Supervised By

Dr. Ahmad Magdy

Dr. Ahmad Nasser

2021

ACKNOWLEDGMENT

First of all, we would like to thank **ALLAH** almighty for giving us strength and patience to go through till finishing our project and reaching these results.

We would also like to express our gratitude and appreciation to the upcoming people, without whom we would not have been able to complete this project, and without whom we would not have made it through our bachelor's degree:

- **Dr. Ahmed Magdy** and **Dr. Ahmed Nasser**, our supportive and patient supervisors and mentors who helped us alot through this project with their advice and experience.
- **Assoc. Prof. Mohammed Nabil**, Head of Electrical Engineering Department.
- **Our families and friends**, who always give us alot of love and support.

SUMMARY

In the era of smart cities, there are a plethora of applications where the localization of indoor environments is important, from monitoring and tracking in smart buildings to proximity marketing and advertising in shopping malls. The success of these applications is based on the development of a cost-efficient and robust real-time system capable of accurately localizing objects. Accurately and efficiently locating objects is a major challenge in indoor environments. Recent advancements in the Internet of Things (IoT) along with novel wireless technologies can alleviate the problem. Small-size and cost-efficient IoT devices which use wireless protocols can provide an attractive solution. In addition to using RSSI in localization, CSI derived from WiFi signals can be used in gait-based identity recognition and device-free human detection which are topics that gained tremendous attention in recent years since they are key enablers of building smart environments. WiFi-based approaches are more desirable with the contactless and non-line-of-sight nature when compared with vision-based and wearable sensor-based solutions.

Taking the mentioned above into consideration, we developed four systems, the first is a localization system using RSSI with the fingerprinting technique to estimate the target's position without having to estimate the distances. The second is an intrusion detection system, the third is a user identification system using the user's own gait, and the fourth is a joint system that combines the intrusion detection system and the user identification system in one system.

TABLE OF CONTENTS

ACKNOWLEDGMENT	ii
SUMMARY	iv
TABLE OF CONTENTS	vi
LIST OF TABLES	ix
LIST OF FIGURES	x
NOMENCLATURE	xii
ABBREVIATIONS	xv
1 INTRODUCTION	1
1.1 WiFi Sensing	1
1.2 Main Applications on WiFi Sensing	1
1.3 Main Advantages of WiFi Sensing	2
1.4 Received Signal Strength (RSS)	2
1.5 Channel state Information (CSI)	2
1.6 Motivation	3
1.7 List of Technologies Used	3
1.8 Objectives	4
1.9 Thesis Structure	4
2 WIFI SENSING TECHNIQUES	5
2.1 RSSI	5
2.2 CSI	7
2.2.1 Radio signal propagation	7
2.2.2 CSI Description	9
2.2.3 Limitations and Errors of WiFi Systems	10
2.2.4 CSI based applications	11
2.3 CSI vs. RSSI	12

TABLE OF CONTENTS

3 IMPLEMENTATION	14
3.1 IWL 5300 Card and Linux CSI Tool	14
3.2 IWL5300 Card Installation	15
3.3 Channel State Information Tool Installation	16
3.3.1 Prerequisites	17
3.3.2 Build and Install the Modified Wireless Driver	17
3.3.3 Install the Modified Firmware	17
3.3.4 Build the Userspace Logging Tool	17
3.3.5 Enable Logging and Test	17
3.4 How To Use the CSI Tool for Linux	18
3.5 Realtime visualization and prediction using python server	18
4 INTRUSION AND HUMAN PRESENCE DETECTION	19
4.1 Introduction	19
4.2 Related Work	20
4.3 Intrusion and Human Presence Detection in Different Scenarios	21
4.3.1 Controlled Scenario	21
4.3.2 Uncontrolled Scenario	21
4.4 Intrusion and Human Presence Detection System	22
4.4.1 Data and Topology	22
4.4.2 Data Visualization	23
4.4.3 Data Preprocessing	24
4.4.4 Feature Extraction	25
4.4.5 Data Classification	26
4.4.6 Results and Analysis	27
5 GAIT RECOGNITION AND JOINT TASK	32
5.1 Introduction	32
5.2 Related Work	35
5.2.1 Gait Recognition in the Old School	35
5.2.2 Gait Recognition in the Modern School	36
5.3 Gait Recognition and Joint Task System (Blaze-WI System)	37
5.3.1 Data and Topology	37
5.3.2 Network	39
5.3.3 Results and Analysis	44

TABLE OF CONTENTS

6 LOCALIZATION BASED ON RSSI	48
6.1 Introduction	48
6.2 Related Work	49
6.2.1 Wi-Fi Indoor Localization Using Crowdsourcing	49
6.2.2 Camera-Based Indoor Localization	49
6.2.3 Indoor Localization Using Multi-Source Heterogeneous Data	50
6.3 Fingerprinting Method	51
6.3.1 Data Collection Points Arrangement	51
6.3.2 RSSI Fingerprint Data Organization	53
6.4 Localization System	54
6.4.1 Data Collection	54
6.4.2 Mobile Application	55
6.4.3 Data Visualization	57
6.5 Results and Discussion	59
6.6 Future Vision and Applications	60
6.6.1 Retail	61
6.6.2 Transportation	61
6.6.3 Warehousing and Logistics	62
6.6.4 Manufacturing	62
7 CONCLUSIONS	63
7.1 Conclusions	63
7.2 Technical Future Vision	64
REFERENCES	66

LIST OF TABLES

2.1	The key differences between CSI and RSSI.	13
5.1	Full network	43
5.2	Comparison with other systems with 6 users	46
5.3	Comparison of Blaze-Wi with different datasets	47
6.1	The structure of RSSI data.	53

LIST OF FIGURES

2.1	RSSI measurements corresponding to different WiFi Access Point in a fixed location	7
2.2	Radio signal propagation in the indoor environment	8
2.3	Example of a MIMO system.	9
2.4	An analogous illustration of RSS and CSI.	12
3.1	Image shows SNR of the 30 subcarriers of each TX and RX connection from our real-time visualization system.	18
4.1	Intrusion Detection in Different Scenarios	21
4.2	Intrusion and human presence detection system design.	22
4.3	Configuration of the topology test.	23
4.4	CSI exhibits different patterns when no human is present or a human is present and moving (a) No movement (b) Movement (c) Presence and movement.	24
4.5	The effect of the Gabor filter on the CSI data (a) No movement (b) Movement.	26
4.6	The confusion matrix for DBSCAN technique (a) SVM (b) KNN.	29
4.7	The confusion matrix for FFT technique (a) SVM (b) KNN.	29
4.8	The confusion matrix for Butterworth low pass filter (a) SVM (b) KNN.	29
4.9	The confusion matrix for Gabor filter (a) SVM (b) KNN.	30
4.10	The system results by CNN(a) the confusion matrix (b) the classification report.	30
4.11	Comparison between the results of all models.	31
5.1	The general WiFi sensing system.	35
5.2	Blaze-WI system design.	37
5.3	Presence and movement.	38
5.4	Configuration of the topology test.	39
5.5	Packet explanation.	39
5.6	Blaze-1D block (left) and Double-1D blaze (right).	40
5.7	Types of convolution layers and the separable depthwise convolution.	41

LIST OF FIGURES

5.8	Types of convolution.	42
5.9	The gait-based identification system using our collected dataset for six volunteers (a) the confusion matrix, and (b) the classification report. . .	45
5.10	The gait-based identification on WIDAR 3.0 dataset for six volunteers (a) the confusion matrix, and (b) the classification report.	46
5.11	The joint task gait-based identification and intrusion task on our dataset for six volunteers (a) the confusion matrix, and (b) the classification report.	47
6.1	Framework of Wi-Fi localization based on RSSI fingerprint.	51
6.2	Schematic diagram of grid data collection in localization area.	52
6.3	The process of RSSI data query and fingerprint feature vector construct.	54
6.4	Localization system design.	54
6.5	Topology.	55
6.6	Mobile application screens (a) 1 st Screen, (b) and (c) 2 nd Screen.	57
6.7	Data visualization graphs (a) RSS recorded for point (0,0), (b) RSS recorded for point (0,3), (c) RSS recorded for point (2,2), (d) RSS recorded for point (3,4).	58
6.8	Comparison between three models accuracies.	59
6.9	Confusion matrix (a) SVM “rbf”, (b) SVM “poly”, (c) kNN	60

NOMENCLATURE

$P_r(d)$	The received power at RX.
$P_r(d_0)$	The transmitted power at TX.
$G_t(d)$	The sender side antenna electric power gain.
$G_r(d)$	The receiver side antenna electric power gain.
$P_r(d_0)$	The power at far-field distance.
d_0	The reference distance (far-field distance).
d	The transmitter-receiver distance.
λ	Wave length.
L	The propagation loss.
γ	The path loss coefficient.
σ	Standard deviation.
X_σ	The Gaussian random variable. into account the noise contribution.
k	The subcarrier index.
y_k	The received signal.

x_k	The transmitted signal.
N_{RX}	The number of receiver antennas.
N_{TX}	The number of transmitter antennas.
H_k	denotes the CSI matrix of the subcarrier k .
h_k^{PQ}	the CSI data between the P^{th} transmitter antenna and Q^{th} receiver antenna of the subcarrier with index k^{th} .
$d_{i,j,n}$	the path length from the i^{th} transmit antenna to the j^{th} receive antenna of the n^{th} path.
f_k	The carrier frequency.
τ_i	The time delay from Cyclic Shift Diversity (CSD) of the i^{th} transmit antenna.
ρ	The Sampling Time Offset (STO).
η	The Sampling Frequency Offset (SFO).
$q_{i,j}$ and $\xi_{i,j}$	The amplitude attenuation and phase shift of the beamforming matrix.
N_{ap}	Number of samples.
l	New Feature.
T	Transformation matrix.

S	Transformed matrix.
W	Feature weights.
L	Number of the original feature.
C_i	Cumulative contribution rate.
i	Number of features.
C_c	Threshold of cumulative contribution rate.
CSI	5 seconds of CSI collected data.
Blaze-Wi	The network.
Y	The output of the last layer in Blaze-Wi.
$prob$	The probability distribution.
$softmax$	The softmax function.
$G_{i,j}$	The number of fingerprinting grids.

ABBREVIATIONS

<i>RSS</i>	Received Signal Strength.
<i>RSSI</i>	Received Signal Strength Indicator.
<i>CSI</i>	Channel State Information.
<i>RF</i>	Radio Frequency.
<i>RFID</i>	Radio Frequency Identification.
<i>GSM</i>	Global System for Mobile Communications.
<i>AP</i>	Access Point.
<i>TX</i>	Transmitter.
<i>RX</i>	Receiver.
<i>OFDM</i>	Orthogonal Frequency Division Multiplexing.
<i>LDPL</i>	Log-normal Distance Path Loss.
<i>LoS</i>	Line of Sight.
<i>NLoS</i>	Non Line of Sight.
<i>IEEE</i>	Institute of Electrical and Electronics Engineers.

<i>MIMO</i>	Multiple-Input and Multiple-Output.
<i>CFR</i>	Channel Frequency Response.
<i>NICs</i>	Network Interface Cards.
<i>CFO</i>	Carrier Frequency Offset.
<i>SFO</i>	Sampling Frequency Offset.
<i>CSD</i>	Cyclic Shift Diversity.
<i>STO</i>	Sampling Time Offset.
<i>ADC</i>	Analog to Digital Converter.
<i>MAC</i>	Media Access Control.
<i>CIR</i>	Channel Impulse Response.
<i>IWL</i>	Intel Wireless Link.
<i>PCIe</i>	Peripheral Component Interconnect Express.
<i>BIOS</i>	Basic Input/Output System.
<i>NVRAM</i>	Non-Volatile Random-Access Memory.
<i>IP</i>	Internet Protocol.
<i>SNR</i>	Signal to Noise Ratio.

<i>EMD</i>	Empirical Mode Decomposition.
<i>EIH</i>	Effective Interference Height.
<i>BP</i>	Back Propagation.
<i>LTS</i>	Long Term Support.
<i>DBSCAN</i>	Density-Based Spatial Clustering of Applications with Noise.
<i>FFT</i>	Fast Fourier Transform.
<i>DFT</i>	Discrete Fourier transform.
<i>PDE</i>	Partial Differential Equations.
<i>PCA</i>	Principal Component Analysis.
<i>SVM</i>	Support Vector Machine.
<i>kNN</i>	k-Nearest Neighbors.
<i>TP</i>	True Positive.
<i>TN</i>	True Negative.
<i>FN</i>	False Negative.
<i>FP</i>	False Positive.
<i>IMU</i>	Internal Measurement Units.

<i>IoT</i>	Internet of Things.
<i>DWT</i>	Discrete Wavelet Transform.
<i>CWT</i>	Continuous Wavelet Transform.
<i>SAC</i>	Sparse Approximation based Classification.
<i>GPS</i>	Global Positioning System.
<i>ToA</i>	Time of Arrival.
<i>TDoA</i>	Time Difference of Arrival.
<i>AoA</i>	Angle of Arrival.
<i>MDS</i>	Multidimensional Scaling.
<i>PM</i>	Propagation Model.
<i>CPs</i>	Crowdsourcing Point.
<i>SVD</i>	Singular Value Decomposition.
<i>POM</i>	Probabilistic Occupancy Map.
<i>CRLB</i>	Cramer-Rao Lower Bound.
<i>UWB</i>	Ultra Wide Band.
<i>FM</i>	Frequency Modulation.

MU Mobile Device.

SSID Service Set Identifier.

Chapter 1

INTRODUCTION

1.1 WiFi Sensing

In light of all these tremendous technological developments, there has been great progress in the role of wireless signals, so that it is not limited to the role of communications only, but also includes applications of remote sensing, especially indoors. In indoor environments, wireless signals often propagate via both the direct path and multiple reflections and scattering paths, resulting in multiple aliased signals superposing at the receiver. Since physical space restricts the propagation of wireless signals, wireless signals, in turn, transmit information that characterizes the environment through which they pass.

1.2 Main Applications on WiFi Sensing

From the information has been taken from wireless signals propagation about the surrounding environment the objects surrounding (e.g. furniture and walls) can be analyzed and also for human activities (e.g. position, presence, gait, activity recognition, gesture recognition, vital signs, intrusion detection and so on). And the applications for that are several. For example, in the field of medicine, there are many researches that have been developed about elderly people tracking systems, especially in light of the increasing number of deaths among the elderly due to the slow detection of sudden accidents such as falls, disturbances, etc.

There is also very important research that has been developed in vital signs-contactless monitoring. That is also a very hot topic in the medical field due to the emergency con-

ditions of a covid-19 pandemic. This topic discusses the application that should measure the vital signs (e.g. respiration and heart rate) accurately in contactless connection. Not only that but there are also applications in the field of security and smart homes systems, etc.

1.3 Main Advantages of WiFi Sensing

Compared with the traditional sensors (e.g. cameras [1] and wearable devices [2]), WiFi sensing gives more safety, privacy and less cost. The reason is that the wireless signals can provide long-range coverage in a range of residential and commercial environments without the need to install a lot of sensors everywhere. Additionally, the wireless signals can not generate images for the place that is covering, unlike cameras, which makes it the perfect solution to protect privacy. Moreover, all these traditional approaches share the requirement of infrastructure installation in the area of interest, and also they have a high installation cost. The advantage of the transmission characteristics of opportunistic WiFi signals in wireless channels is taken by the research of WiFi-based sensings, such as Received Signal Strength (RSS) and Channel State Information (CSI).

1.4 Received Signal Strength (RSS)

Since RSS is only a description of the received power (strength) [3]. RSS acts as a common proxy for channel quality and is accessible in many wireless communication technologies including RFID, GSM, WiFi and Bluetooth. Theoretically, RSS transmitted by an Access-point (AP) can be used to estimate the propagation distance, meaning that the weak strength of a WiFi AP gives an indicator for a long distance and vice versa. Also, a set of RSS can be taken from multiple APs as fingerprints for each location, or infer human motions from RSS fluctuations which are called the fingerprint method and this will be described later.

1.5 Channel state Information (CSI)

On the opposite side, the detailed propagation of signals from the transmitter (TX) to receiver (RX) through multiple paths at the granularity of Orthogonal Frequency Division Multiplexing (OFDM) subcarriers is described by the CSI, both amplitude and phase information for each propagation path is contained by the CSI. By analyzing the changed

signal paths and channel state on CSI impacted by moving targets, more accurate and robust intrusion detection and gait based identity identification solutions can be achieved.

1.6 Motivation

The reason why we chose the topic of WiFi sensing is that WiFi sensing is nowadays a trending technology and the interests of founders are focused on that due to its advantages previously discussed. So, it can get back for us with huge commercial benefits, especially, it can be turned into a startup company.

1.7 List of Technologies Used

1. Software Packages

- Fluter mobile development kit
- Pytorch
- Tensorflow/Keras
- Tensorflow Lite
- Socket
- PyQtGraph

2. Programming Languages

- Python
- Dart
- C
- Bash script
- MATLAB

3. Hardware

- Dell Latitude e6430
- HP Compaq 2510p
- Intel 5300 Wi-Fi card

- Wireless Router TL-WR940N
- Smartphone devices

1.8 Objectives

The scope of this thesis is, primarily, uses WiFi sensing. Specifically, the objectives of the research work presented in this thesis cover the following:

- Intrusion and human presence detection system based on CSI
- Gait recognition system based on CSI
- A joint between Intrusion Detection and Gait Recognition system
- Localization system based on RSS

1.9 Thesis Structure

The previous objectives of this thesis are described in seven chapters. In chapter 2, we will introduce a description about wifi sensing techniques . In chapter 3, we will describe the implementation of the system that we have used to collect the CSI. Chapter 4 describe Intrusion and human presence detection based CSI and the techniques that used to implement it. Chapter 5 continue to talk about csi based applications such as Gait recognition also will describe the combining Intrusion detection and Gait recognition in a joint task. Chapter 6 is talking about Localization system based RSSI. Chapter 7 provide a conclusion about the project.

Chapter 2

WIFI SENSING TECHNIQUES

Wi-Fi technology has strong potentials in indoor and outdoor sensing applications, it has several important features which makes it an appealing option compared to other sensing technologies, as we mentioned before in chapter 1. WiFi sensing is an emerging concept that uses WiFi radios as sensors [4]. In this chapter, we present preliminary knowledge of WiFi signal. Specifically, we introduce two numerical “sensor” readings, namely Received Signal Strength Indicator (RSSI) and Channel State Information (CSI).

2.1 RSSI

Received Signal Strength Indicator (RSSI) defines the relative power strength of the received signal. In IEEE 802.11 standard, RSSI is internally used to reflect a link quality [5]. To calculate the received signal strength we will use friis-equation to express the received and transmitted power from TX and RX antenna as the following formula.

$$P_r(d) = \frac{P_t \cdot G_t \cdot G_r \cdot \lambda^2}{(4\pi)^2 \cdot d^2 \cdot L} \quad (2.1)$$

by multiplying the formula by $(\frac{d_0^2}{d^2})$, where d_0 is the reference distance (far-field distance) which depends on antenna technology and d is setting the transmitter-receiver distance, G_t is Sender side antenna electric power gain and G_r is Receiver side antenna electric power gain and λ is the wavelength.

L represents other losses that is not associated with the propagation loss. The parameter L may include system losses like loss at the antenna, transmission line attenuation, loss at various filters etc. The factor L is usually greater than or equal to 1 with $L = 1$ for

no such system losses.

$$P_r(d) = \frac{P_t \cdot G_t \cdot G_r \cdot \lambda^2}{(4\pi)^2 \cdot d_0^2 \cdot L} \left(\frac{d_0}{d}\right)^2 = P_r(d_0) \cdot \left(\frac{d_0}{d}\right)^2 \quad (2.2)$$

where $P_r(d)$ is the received power at RX, $P_r(d_0)$. is the power in farfeild distance. to take into account stronger attenuation than only caused by distance (e.g., walls, . . . etc.) use lager exponent ($\gamma > 2$), where γ is the path loss coefficient. So, the formula should be like following:

$$P_r(d) = P_r(d_0) \cdot \left(\frac{d_0}{d}\right)^\gamma \quad (2.3)$$

to represent power received in RX $P_r(d)$ in [dB] form:

$$P_r(d)[dB] = P_r(d_0)[dB] + 10\gamma \log\left(\frac{d_0}{d}\right) \quad (2.4)$$

take obstcales into account by random variation:

- Add Gaussian random variable with 0 mean, variance σ^2 to dB representation.
- Equivalent to multiplying with a lognormal distributed $r.v$ in metric units Lognormal fading.

$$P_r(d)[dB] = P_r(d_0)[dB] + 10\gamma \log\left(\frac{d_0}{d}\right) + X_\sigma[dB] \quad (2.5)$$

Based on Eq. 2.5, we can roughly get the relationship between distance and power strength. However, in a complex indoor environment, the multipath effect [6]will greatly distort the model, making it almost impossible to infer location from Eq. 2.5 . Fig. 2.1 depicts the RSSI measurements corresponding to different WiFi APs in a fixed location. We can see that RSSI can fluctuant heavily, making it an unreliable indicator.

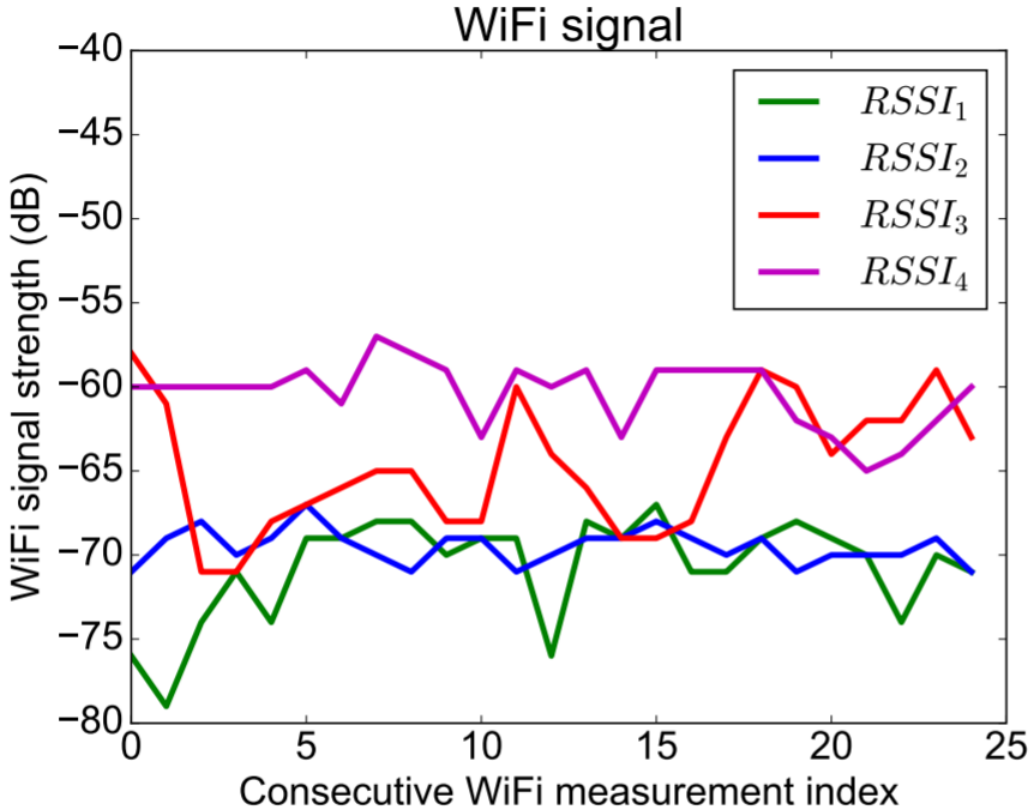


Figure 2.1: RSSI measurements corresponding to different WiFi Access Point in a fixed location .

2.2 CSI

2.2.1 Radio signal propagation

In conventional wireless communication systems, various factors such as scattering, reflection, or diffraction by the physical environment can influence the transmitted radio signal that reaches the receiver. Moreover, the transmitted signal reaches the receiving antenna by many paths (also known as multi-path propagation) due to some obstacles that block the Line-Of-Sight (LOS) path and also the reflections from the physical environment (see Fig. 2.2). These multipath components contain different time delay, amplitude attenuation, and phase shift information, which makes it possible to identify the various situations in the environment such as human presence, activity, gesture and so on.

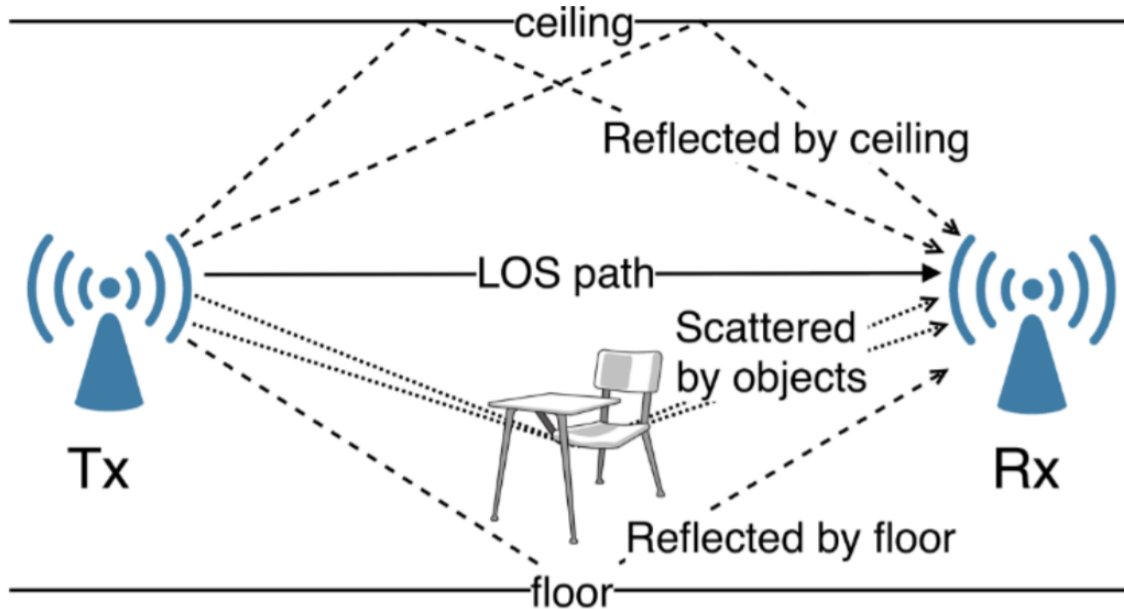


Figure 2.2: Radio signal propagation in the indoor environment .

Commonly, a typical Wi-Fi (IEEE 802.11a/g/n) system increases the data transfer capacity of the link by multiplexing data streams over the multiple transmit antennas to multiple receive antennas. Specifically, this type of arrangement is also called a Multiple-Input and Multiple-Output (MIMO) communication system. By using this technology, it is possible to increase the diversity gain, array gain, and multiplexing gain, while reducing the co-channel interference [7], which typically contains M antennas at the transmitter and N antennas at the receiver, each receiver antenna receives the LOS signal and also a fraction of the signal from other propagation paths. As shown in Fig. 2.3, each receiver antenna receives not only the direct signal intended for it but also the signals from other propagation paths. Based on the incoming signal that contains amplitude and phase, the receiver measures discrete Channel Frequency Response (CFR) in two domains: CFR of time and CFR of frequency. Afterwards, the system can generate Channel State Information (CSI) as a matrix with the dimension of NM .

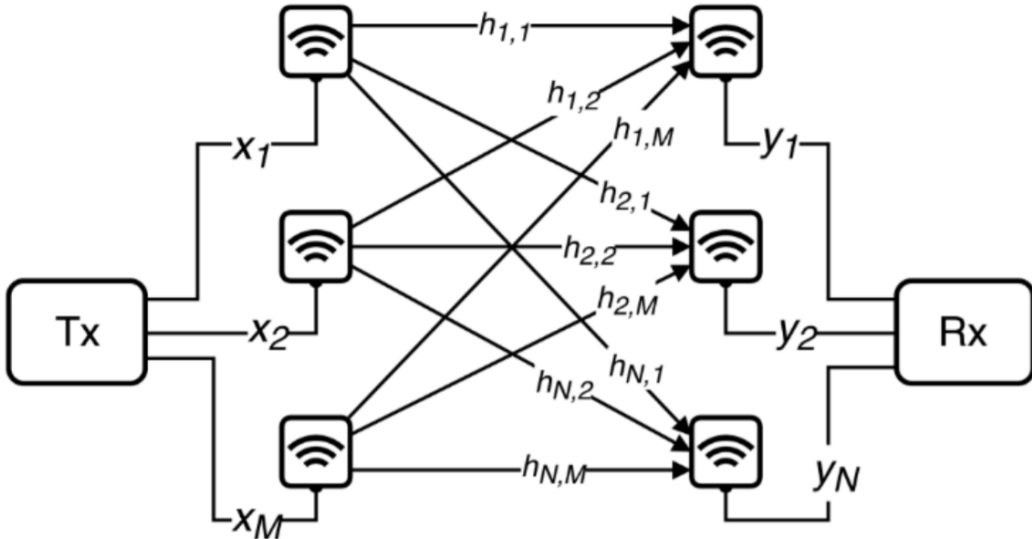


Figure 2.3: Example of a MIMO system.

2.2.2 CSI Description

Channel state information (CSI) describes the known channel properties of a communication link from the physical layer that is more stable and more capable of providing fine-grained information in complex environments. This information illustrates how a radio signal propagates from the transmitter to the receiver and represents the combined effects of scattering, weak environment (Fading, multipath or shadowing Fading), distance attenuation (Power Distance Decay of). Commonly, Wi-Fi (IEEE 802.11a/g/n) systems use Orthogonal Frequency Division Multiplexing (OFDM) to divide the overall spectrum band into many small and partially overlapped frequency bands called subcarriers for high-performance wireless communications [8]. In the OFDM systems, CSI contains the complex values of the CFR which represents the channel properties of each subcarrier. In general, for the narrowband flat fading channel (a Wi-Fi channel in the 2.4 GHz/5GHz band) with MIMO, the CSI is represented in terms of the channel transmission matrix H by

$$y_k = H_k x_k + n_k \quad (2.6)$$

where k is the subcarrier index, $y_k \in R^{N_{RX}}$ and $x_k \in R^{N_{TX}}$ are the received and transmitted signals, respectively, N_{RX} is the number of receiver antennas, N_{TX} is the number of transmitter antennas, n_k is the noise vector, and $H_k \in C^{N_{RX}N_{TX}}$ denotes the CSI matrix

of the subcarrier k

$$H_k = \begin{pmatrix} h_k^{11} & h_k^{12} & h_k^{13} & \dots & h_k^{1N_{RX}} \\ h_k^{21} & h_k^{22} & h_k^{23} & \dots & h_k^{2N_{RX}} \\ \vdots & \vdots & \vdots & \ddots & \vdots \\ h_k^{N_{TX}1} & h_k^{N_{TX}2} & h_k^{N_{TX}3} & \dots & h_k^{N_{TX}N_{RX}} \end{pmatrix} \quad (2.7)$$

where h_k^{PQ} contains the CSI data between the P^{th} transmitter antenna and Q^{th} receiver antenna of the subcarrier with index k^{th} .

The h_k^{PQ} is a complex value, which have an amplitude of $|h_k^{PQ}|$ and phase $\angle h_k^{PQ}$ so the h_k^{PQ} can be represented as

$$h_k^{PQ} = |h_k^{PQ}| e^{j\angle h_k^{PQ}} \quad (2.8)$$

The channel matrix for k^{th} subcarrier H_k can be estimated by dividing the output signal with a known sequence of input also known as a pilot. The channel matrix shows how the input symbol is affected by the channel to reach the receiver. In OFDM systems, each subcarrier faces a narrow-band fading channel, and by obtaining the CSI for each subcarrier, there will be diversity in the observed channel dynamics. This is the main advantage of using CSI compared to RSS, in which the changes are averaged out over all the WiFi bandwidth and hence cannot capture the change at certain frequencies. In some commercial network interface cards (NICs), such as Intel NIC 5300 the CSI can be collected using the tool provided in [9].

2.2.3 Limitations and Errors of WiFi Systems

The amplitude of CSI is generally a reliable metric to use for feature extraction and classification, although it can change with transmission power and transmission rate adaptation. By using filtering techniques, the burst noise can be reduced [10]. However, in contrast to amplitude, the phase of the WiFi system is affected by several sources of error such as carrier frequency offset (CFO) and sampling frequency offset (SFO). The measured baseband-to-baseband CSI is

$$H_{i,j,k} = \sum_n^N a_n(t) e^{-j2\pi d_{i,j,n} f_k / c} \cdot e^{-j2\pi \tau_i f_k} \cdot e^{-j2\pi \rho_i f_k} \cdot e^{-j2\pi \eta(f'_k / f_k - 1) f_k} \cdot q_{i,j} e^{-j2\pi \xi_{i,j}} \quad (2.9)$$

where $d_{i,j,n}$ is the path length from the i^{th} transmit antenna to the j^{th} receive antenna of the n^{th} path, f_k is the carrier frequency, τ_i is the time delay from Cyclic Shift Diversity (CSD) of the i^{th} transmit antenna, ρ is the Sampling Time Offset (STO), η is the Sampling Frequency Offset (SFO), $q_{i,j}$ and $\xi_{i,j}$ are the amplitude attenuation and phase shift of the beamforming matrix. Where the CFO exists due to the difference in central frequencies (lack of synchronization) between the transmitter and receiver clocks. The CFO for a period of 50 μ s of 5GHz WiFi band can be as large as 80KHz, leading to a phase change of 8π . Therefore, the phase changes due to the movement of the body, which is generally smaller than 0.5π , is not observable from phase change. The other source of error, SFO, is generated by the receiver analog to digital converter (ADC). The SFO is also varying by subcarrier index, therefore, each subcarrier faces a different error. Due to the unknown CFO and SFO, using the raw phase information may not be useful. However, a linear transformation is proposed in [11], such that the CFO and SFO can be removed from the calibrated phase. This process is also known as phase sanitization.

2.2.4 CSI based applications

For a WiFi system with MIMO-OFDM, CSI is a 3D matrix of complex values representing the amplitude attenuation and phase shift of multi-path WiFi channels as we discussed before in section 2.2.2 . A time series of CSI measurements capture how wireless signals travel through surrounding objects and humans in time, frequency, and spatial domains, so it can be used for different wireless sensing applications. For example, CSI amplitude variations in the time domain have different patterns for different humans, activities, gestures, etc., which can be used for human presence detection [13–16], fall detection [17–19], motion detection [20, 21], activity recognition [22–26], gesture recognition [27–29], and human identification/authentication [30–32]. CSI phase shifts in the spatial and frequency domains, transmit/receive antennas and carrier frequencies, are related to signal transmission delay and direction, which can be used for human localization and tracking [33, 34]. CSI phase shifts in the time domain may have different dominant frequency components which can be used to estimate breathing rate [35–38]. Different WiFi sensing applications have their specific requirements of signal processing techniques and classification/estimation algorithms. Later, we will discuss some CSI based applications such as user identification and intrusion detection in more detail...

2.3 CSI vs. RSSI

Compared with RSS, CSI is able to depict multipath propagation to a certain extent, making it an upgrade for RSS. Analogously speaking, CSI is to RSS what a rainbow is to a sunbeam. As shown in Fig. 2.4, CSI separates signals of different wavelengths via OFDM, while RSS only provides a single-valued amplitude of superposed paths.

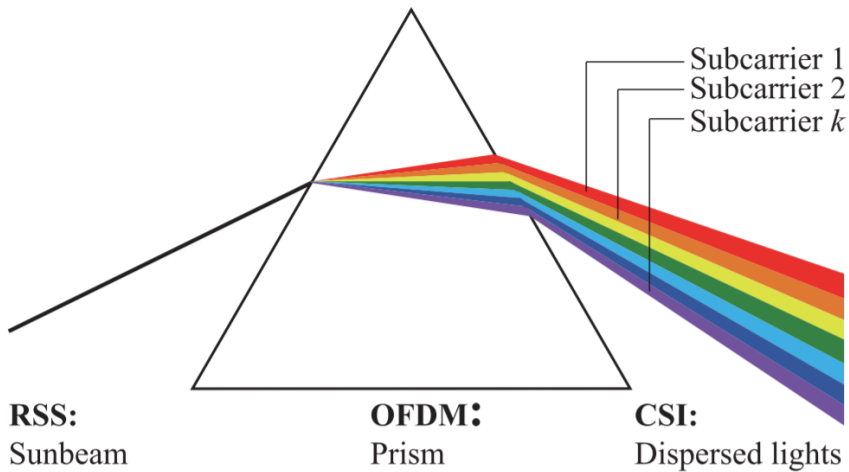


Figure 2.4: An analogous illustration of RSS and CSI.

As physical layer information, CSI conveys channel information invisible in MAC layer RSS. On one hand, CSI estimates CFR on multiple subcarriers, thus depicting the frequency-selective fading of WiFi channels. On the other hand, CSI measures not only the amplitude of each subcarrier but its phase as well. Thus CSI provides richer channel information in the frequency domain. Since CIR is the inverse Fourier transform of CFR, CSI also enables coarse-grained path distinction in the time domain. CSI brings more than richer information. With proper processing, CSI can exhibit site-specific patterns in different environments, while retaining stable overall structure in the same environment. Hence we may extract finer-grained and more robust signal features from CSI via machine learning and signal processing, rather than obtain only a single value by simply adding up the amplitudes over subcarriers (a similar processing approach as RSS). As the following table 2.1 briefly illustrates the key differences between CSI and RSSI.

Table 2.1: The key differences between CSI and RSSI.

Metric	RSSI	CSI
Network layer	<i>MAC layer</i>	<i>Physical layer</i>
Time resolution	<i>Packet size</i>	<i>Multipath signal cluster scale</i>
Frequency resolution	<i>No</i>	<i>Subcarrier scale</i>
Temporal stability	<i>Low</i>	<i>High</i>
Measurement band	<i>RF-band</i>	<i>Baseband</i>
Granularity	<i>Coarse-grained (per packet)</i>	<i>Fine-grained (per subcarrier)</i>
Universality	<i>Almost all wifi devices</i>	<i>Some wifi device</i>

Chapter 3

IMPLEMENTATION

In this chapter, we will describe the implementation of the system that we have used to collect the CSI. This chapter has two parts: hardware setup and installation and software implementation. In the hardware section, we will describe the characteristics and critical points for the installation of the chosen hardware. In the software section, we will go through the steps to install the software for collecting the CSI information.

Hardware Selection

Recall that to select a valid chipset it has to comply with the following two conditions: the operation in 802.11n WiFi protocol and the existence of specialized software that can access the physical layer from the userspace to recover the CSI. Nowadays there are only two known software tools for this kind of WiFi chipsets. The oldest one, developed by Daniel Halperin et al. in 2011 [121], works exclusively for the Intel Wireless Link 5300 (IWL5300) NIC card. In 2015 Yaxiong Xie et al. [122] developed a second tool designed to work for any device with an Atheros manufacturer chipset, installed either in an OpenWRT OS Access Point or NIC card of a laptop.

With the aim of using and testing a system as close to reality as possible, the first approach of this project was to build end-to-end intrusion detection and gait recognition system on top of IWL5300. In the following sections, we will explain the process to install the Intel card and the software to recover the data it gathers.

3.1 IWL 5300 Card and Linux CSI Tool

In this Section, we will pinpoint all the problems found during the installation of the hardware and building up of the setup. Then we will talk about the installation steps of the Linux tool that was developed to work along with it. We will give a user

guide for its utilization and an example of the data representation obtained with it. The Linux software tool for the IWL5300 card computes the CSI at the receiver side when the packets that arrive are sent in 802.11n rates and pass it to higher layers of the operating system, where the user can access it. To do so, there are two main places where to apply software modifications: the operating system and the wireless card firmware. The change in the firmware is transparent to us as we can't see the code, but we are aware of its purpose. The new firmware enables the debug mode in the card. This mode was designed by the chipset developers to check the functioning of the CSI computation, so the chipset will compute it for any packet that arrives with an 802.11n rate. Thanks to the transfer of the code from their side, we are able now to see those values outside the physical layer. On the other hand, there are some changes to the wireless drivers in the operating system, so that the data can arrive at the userspace. These changes will allow logging multiple aspects as well as the data, and to pipe it upstream to the userspace.

3.2 IWL5300 Card Installation

The Hardware installation consists of two main components: the IWL530 wireless card and the laptop where to plug it. There is a third important part, the antennas, and the connectors as it's very rare in Egypt so we have worked on the internal antennas. The main problem with the card, mainly due to its availability in the Egyptian market, is the size to choose from. There is a full-size card and a half-size one. The small one was designed to fit in the newest and more compact laptops, where the big one doesn't fit. The second important feature of any of the cards is that they use a PCIe connector 1 . These two factors will restrict the computer we can choose to install the card. Both size cards should support this tool, but we have only tested it with the full-size one. For this project, we had access to full-size cards, and we bought an old HP Compaq 2510p laptop. Its most interesting specifications are

- Intel Centrino Duo processor.
- Intel PRO/Wireless 3954ABG.
- PCIe connector.

On the laptop side, the critical issue is what is called hardware whitelisting. Some laptops include a list of accepted hardware components. If we substitute one of the native

3.3 Channel State Information Tool Installation

components with a new piece of hardware that is not on the list, the computer will not boot. For the HP computers, and in particular, for this model, we find this problem. We found three different approaches to overcome the whitelist problem:

1. Modify the BIOS changing a bit in the nonvolatile BIOS memory. In a Linux Operating System, we can access this memory by reading the /dev/NVRAM file.
2. Install a modified BIOS that removes the hardware whitelist restriction.
3. Change the card ID so that it matches with one that is in the approved hardware list.

The first and third options are explained in detail in [123]. For the first option, they provide a small program that changes one bit in the BIOS memory space to disable the whitelist check. Unfortunately, this method is not extensible to every HP model, and it didn't work out for the 2510p. The third option seems simple, but it is difficult to find the original table of accepted cards, and the procedure is quite risky. The final solution was to find or build ourselves a modification of the BIOS that bypasses the check. After an intensive search, we have decided to search more for a laptop that supports the intel 5300 and we've found this one Dell Latitude E6430 which has Intel Core i5-3320M and 1 x 4 Gigabyte DDR3 RAM. This laptop supports the IWL5300

3.3 Channel State Information Tool Installation

Now that the laptop can boot, we can install the CSI tool for Linux 121. The only requirement here is to choose a Linux-based Operating System with a supported kernel version between 3.2 and 4.2. For this project, we chose an old Ubuntu distribution, specifically 12.04 with v.3.13 kernels. Be aware of the support that the Ubuntu community provides to the kernel versions [124]. Most of the old versions of the OS will have updated v.4.4 kernels, so the right 12.04 distribution can be found in [125]. Once the Operating system is set up, we can start with the installation of the CSI tool following the instructions in [126]. As indicated, this process has five steps to be performed from the command line, and can be summarized as follows:

3.3.1 Prerequisites

Install the build tools, the Linux development headers according to the kernel version, and the Git client. After this, my recommendation is to follow the first tip and disable the Network Manager to avoid conflicts in the management of the wireless connections. All the configurations can be done with the iw utility from the command line.

3.3.2 Build and Install the Modified Wireless Driver

Obtain the CSI Tool Linux source tree, with the appropriate changes to the wireless driver that match the kernel version. Note: The direct cloning process of the CSI Tool repository took a really long time for this laptop ($> 3h$). The processing capability of the laptop has an important role in this step. To save some time, cloning the repository in one computer with the same kernel version tag, and copying it in the wanted one was proven to work.

In the first tip. This process should resolve without conflicts if we are using a supported kernel version by the tool (like v.3.13). If the merge outputs conflict, we should check we are indeed working with the correct kernel version3. The tool won't work if we ignore this mismatch in the merging. Finally, we have to build and install the modified driver as explained in the instructions. For this laptop, we will get the message can't read the private key after loading the new driver, but it will not affect the functioning of the tool.

3.3.3 Install the Modified Firmware

Substitute the original IWL5300 card firmware with the modified firmware.

3.3.4 Build the Userspace Logging Tool

Consists of building the tool that logs at the userspace the CSI that comes from the driver.

3.3.5 Enable Logging and Test

Finally, we have to unload the driver and reload it enabling the logging capabilities. To enable the different logging possibilities there is a parameter called connector log loaded at the same time as the driver.

3.4 How To Use the CSI Tool for Linux

Connector log indicates the amount and type of information to log. In the code of the tool, there are several masks defined associated with different kinds of information. In principle, this would be enough to set up the tool if we want to compute the CSI for packets coming from an AP. We need to establish an unencrypted connection with an AP and run the following command to start the CSI logging utility: `sudo linux-802.11n-csitool-supplementary/netlink/ log_to_file csi.dat` while pinging on the IP of the transmitter in another terminal. Then, we can compute the CSI from the packets that the AP pings back in 802.11n rates.

3.5 Realtime visualization and prediction using python server

We have to build a script on top of C script which is used to send the data to Matlab for real-time visualization and make it available for python and with some tweaking, on an available Python package called `csiread` we have managed to access the data in realtime as shown in Fig. 3.1 with more than 200 packet per second which offers a lot of applications and we have used it to run our real-time experiments. Access the data through python offers many potential applications due to the huge support of Python's community and the huge number of the available packages.

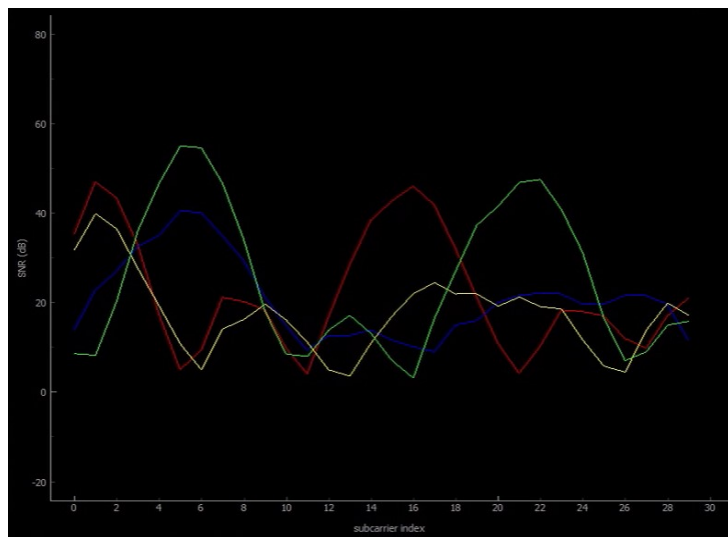


Figure 3.1: Image shows SNR of the 30 subcarriers of each TX and RX connection from our real-time visualization system.

Chapter 4

INTRUSION AND HUMAN PRESENCE DETECTION

4.1 Introduction

Device-free passive detection is an emerging technology to detect whether there exists any (moving) entities in the area of interest without attaching any device to them [118, 119]. It is an essential primitive for various applications including intrusion detection for safety precautions, patient monitoring in hospitals, child and elder care in home, detection of living people in a fire or earthquake, and battlefield military applications, etc. In such applications, users should not be expected to carry any purposed devices for localization or detection.

Therefore, many passive human detection and intrusion systems have been developed based on various technologies, e.g., camera [39], sound [40, 41] and infrared [42]. Camera-based approaches use a camera situated in the monitoring area to capture video screams and analyse them to indicate passive activity recognition. It can, however, only be used in lighting. The line-of-sight (LOS) characteristic is required in all situations. Furthermore, one of its key concerns is the possibility of privacy leakage and high false alarm rate. It is usually required to wear a sensor on the body which might be inconvenient for some people, and other settings are not appropriate for wearing sensors. Also, due to the privacy protection requirement, camera-based or sound-based approaches are usually not desirable for indoor intrusion and human presence detection [43]. Infrared-based systems [42, 44] can achieve good detection accuracy while preserving the privacy of the user. However, the detection

range/angle of infrared is limited, making it difficult to achieve high coverage in practice.

Compared with these approaches, WiFi-based human detection achieves a better trade-off between accuracy and privacy protection. Also, WiFi is already widely available, which means that the extra deployment cost can be minimized. Intrusion detection is a primary and fundamental application in wireless sensing, and recent years have witnessed its rapid development, especially based on CSI provided by off-the-shelf WiFi devices.

4.2 Related Work

FIMD [45] utilizes the observation that the temporal correlation of CSI amplitude will fall dramatically when there is a moving human to achieve intrusion detection. PADS [41] is similar to FIMD [45], but it is the first effort to utilize CSI phase information as well to determine human presence. Deman [46] proposes a method to further detect whether a person is in motion or not by fitting CSI sequence to the sinusoidal breathing model to estimate the primary respiratory rate. If the estimated frequency falls within the normal person's respiratory frequency range, then the system assumes that a static person exists.

Omni-PHD [47] uses fingerprints and Empirical Mode Decomposition (EMD) algorithm to detect intrusion in all directions. Despite that these works have achieved high accuracy, their performance cannot be guaranteed with a relatively low sampling rate of 15-20Hz and they can hardly be transplanted to embedded devices for commercial use.

RR-Alarm [48], by reusing the existing Wi-Fi signals, is able to detect human intrusion in real-time, at the same time, requiring no additional facilities installation. By utilizing the Doppler effects incurred by human motion on multiple Wi-Fi devices, RR-Alarm is not only able to accurately detect the intrusion without any extra-human efforts but also avoids a large number of false alarms caused by the human motion from outside the house. PetFree [49] on the other hand uses fine-grained Channel State Information (CSI) of WiFi signals to detect whether there is a human or a pet in the monitoring area. The basic idea of PetFree is to use the Effective Interference Height (EIH) differences between humans and pets. In another literature, TWMD system [50] is a new detection idea that expands the dimension and quantity of features and then it builds Back Propagation (BP) neural network to obtain the mapping relationship between multiple features and detection results. This detection scheme can avoid the system instability caused by improper feature selection and insufficient number of features. At the same time, in

4.3 Intrusion and Human Presence Detection in Different Scenarios

order to enhance the reliability of TWMD in low SNR environments, the output features of BP neural network of each antenna are merged.

4.3 Intrusion and Human Presence Detection in Different Scenarios

In our work, we use WiFi signals to detect Humans in different Scenarios, and these Scenarios are illustrated in Fig. 4.1.

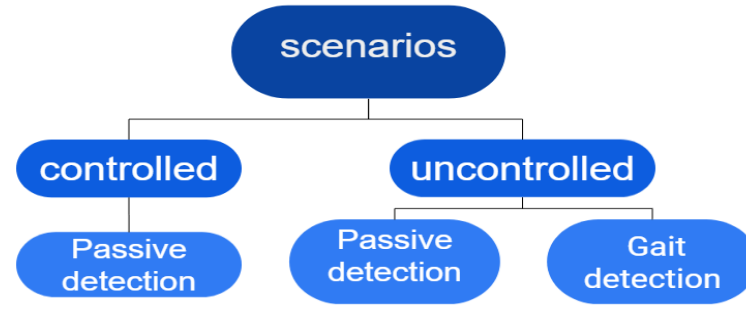


Figure 4.1: Intrusion Detection in Different Scenarios .

4.3.1 Controlled Scenario

In this Scenario the place is being empty for a period of time. In other words the presence of humans in this place is controlled so we have two status for this place which are dynamic and static.

In the dynamic status the presence of human is allowed while in the static status the presence of human is forbidden so we tell the system that in this period of time if you detect that there is a presence of human so this could be an intruder, The controlled place could be a bank, cinema, mall,...etc.

4.3.2 Uncontrolled Scenario

In this Scenario the place there isn't a routine in which the place is dynamic or static so we use the first Scenario if we are sure that this place will be static for a certain period of time but most of the time we use gait detection in which the system knows the gait for each individual whose presence is allowed we will discuss this later, The uncontrolled place could be a house, hotel...etc.

4.4 Intrusion and Human Presence Detection System

As shown in Fig. 4.2 a complete illustration of the intrusion and human presence detection system design, which will be analysed through the following steps:

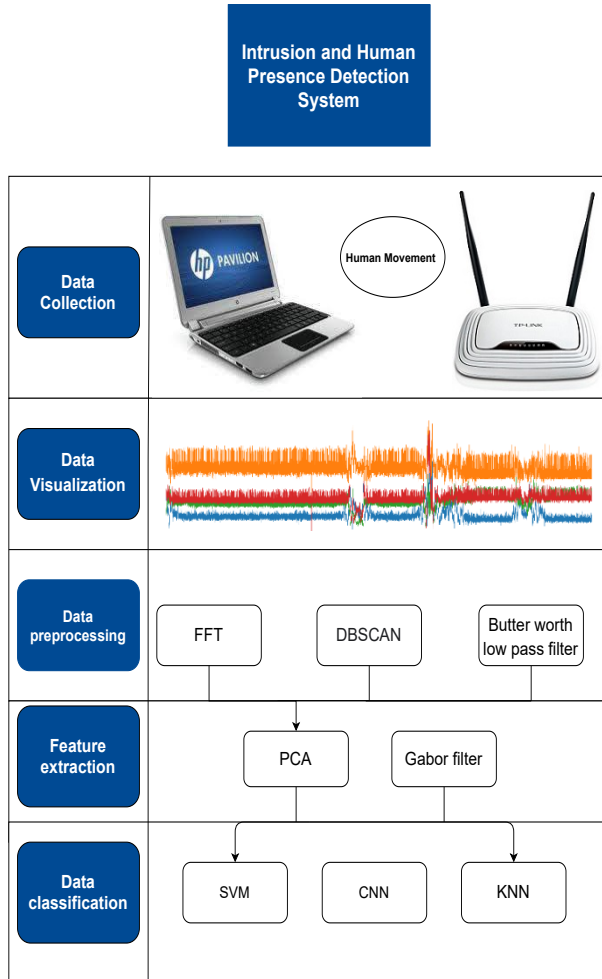


Figure 4.2: Intrusion and human presence detection system design.

4.4.1 Data and Topology

A- Hardware

A Dell latitude E5400 laptop operating on Linux 14.04 LTS operating system has been used. It's equipped with Intel 5300 wireless NIC. A Linux 802.11n CSI Tool has been installed on the laptop. A three-antenna access point (AP) operating at 2.4 GHz band has been used.

B- Topology

As shown in Fig. 4.3, the test environment consisted of a regular $4 \times 3.5 m^2$ room. The environment contains a bed, 2 tables and a chair. The laptop and APs are fixed at the opposite sides of the room so they will cover the full room and will be sensitive to any movement.

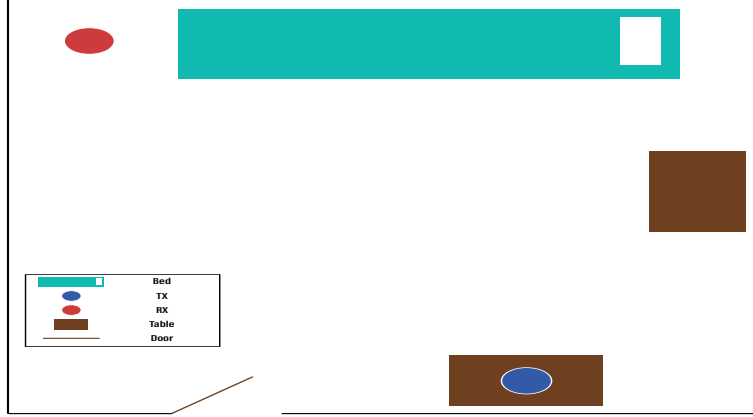


Figure 4.3: Configuration of the topology test.

C- Data Collection

In this work, the participant is asked to enter the room and walk inside it while the system was collecting the CSI data for about 20 minutes. The room then closed without anyone inside it . At the same time the laptop receives the packets from the access point then extracts the CSI measurements and saves it in a file named after the participant's name and the task name. The sampling rate is 90Hz. Each second the collected data shape is [90, 30, 2, 2] where 90 is the number of packets, 30 is the number of subcarriers, 2 is the number of TX antennas, and the last 2 is the number of RX antennas.

4.4.2 Data Visualization

CSI exhibits different patterns when the area of interest is vacant or when a human moves. Fig. 4.4 illustrates the properties of CSI of one link for device-free presence detection, in which the *X – axis* represents the packets over time and the *Y – axis* represents the amplitude of the subcarrier. Different colors represent different connections between TX and RX antennas. Fig. 4.4(a) illustrates the amplitude of subcarrier number "11" in the link when no human is present in the area of interest. Its pattern is quite different from the CSI patterns when a human moves, as Fig. 4.4(b) shows. Human presence can

4.4 Intrusion and Human Presence Detection System

be detected through statistical analysis or machine learning classification model on CSI patterns. As also shown in Fig. 4.4(c) CSI contains meaningful data about the surrounding area which needs mining to extract them.

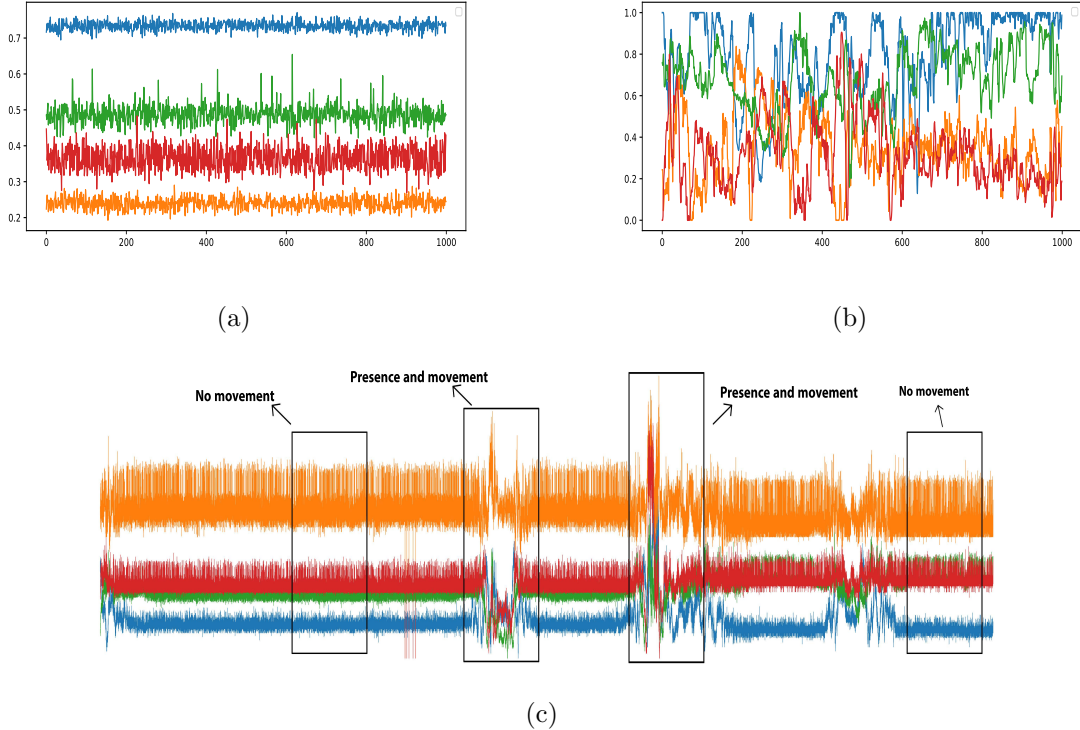


Figure 4.4: CSI exhibits different patterns when no human is present or a human is present and moving (a) No movement (b) Movement (c) Presence and movement.

4.4.3 Data Preprocessing

CSI is usually taken to be multi-interfering due to noise and internal state transitions during transmission and reception(e.g., changes in TX power or transmitting rate adaptation, which may introduce high amplitude impulse and burst noise). Therefore, we process raw signals by using one of the following techniques:

A- DBSCAN

Observations show that raw CSI data have noise. We apply the DBSCAN(Density-Based Spatial Clustering of Applications with Noise) algorithm to detect and remove the noise. DBSCAN [57] is a density-based clustering algorithm, which groups points that are closely packed together and mark as outliers that lie alone in low-density regions. It does not require to specify the number of clusters a priori and can be used to detect and remove noise. DBSCAN is performed on the dataset of each TX-RX link.

4.4 Intrusion and Human Presence Detection System

B- FFT

As we discussed before that CSI data have noise due to environmental changes. We apply the FFT algorithm to remove this noise. the Fast Fourier transform (FFT) [51, 52] is one of the most important algorithms that have changed the world fundamentally. It offers a computationally fast and efficient way for DFT calculation. It's a notable piece of technology in digital communication, satellite communication, TV technology, data analysis, audio compression and image compression. It's also a numerical technique to solve PDEs (Partial Differential Equations) in scientific computing. In data science, the FFT can be used to denoise data.

C- Butterworth Low Pass Filter

We also apply Butterworth low pass filter to reduce noise. Butterworth low pass filter [120] is a digital filter that effectively reduces the unwanted higher-order frequency components in a signal.

4.4.4 Feature Extraction

Considering there are N_{ap} (Number of samples) TX-RX pairs and each pair of TX-RX contains $N_{TX} \times N_{RX}$ links, and each link has N subcarriers, thus each CSI sample has $N_{ap} \times N_{TX} \times N_{RX} \times N$ dimensions. In our dataset in the room, a CSI sample contains 120 dimensions. High dimensionality causes time complexity. As each dimension may have a different contribution to human presence detection. so we use one of the following techniques to extract the feature:

A- PCA

We apply PCA (Principal Component Analysis) algorithm to extract the most contributing features and reduce the dimensionality of CSI data. PCA [55] converts a set of possibly correlated variables into a set of linearly uncorrelated variables, called principal components, through orthogonal transformation. The first principal component has the largest possible variance, and each succeeding component in turn has the highest variance possible and orthogonal to the preceding components.

For the goal of dimensionality reduction, PCA is to find l new features, with each one being a linear combination of the original features, so that the new features can reveal the nature of the original data and compress them. Through PCA on the CSI matrix H , we obtain the transformation matrix T , the transformed matrix S and the feature

4.4 Intrusion and Human Presence Detection System

weights $W = (w_1, w_2, \dots, w_L)$ in descending order, wherein L is the number of the original features. The cumulative contribution rate C_i till feature i is defined as

$$C_i = \frac{\sum_{j=1}^i w_j}{\sum_{j=1}^L w_j} \quad (4.1)$$

If the cumulative contribution rate of the first l features, i.e. C_l , is greater than the predefined threshold C_c , we take the first l features, i.e. (w_1, w_2, \dots, w_l) , as the extracted features. The first l rows of the transformed matrix S constitute the principal component matrix R , which will be used for the subsequent model training, presence detection. In our dataset in the room, a CSI sample contains 120 dimensions and we reduced them to 15.

B- Gabor Filter

We also applied the Gabor filter as a feature extractor to extract the most contributing features from the CSI data. The Gabor filter [56] feature extraction process starts with the application of a two-dimensional Gabor filter which is applied to each signal individually. The process is guided by Gabor's uncertainty principle, which states that the product of frequency resolutions and time must be greater than a constant. The principle aids in a better selection of orientations and frequencies. The principle also implies that frequency and spatial measurements must define a rectangular shape in Fourier space having an area $\geq \frac{\pi}{4}$. Fig. 4.5 illustrates the effect of the Gabor filter on the CSI data.

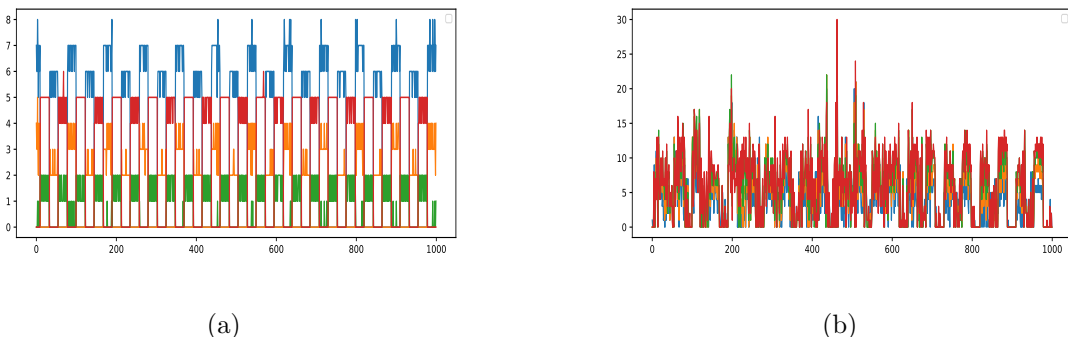


Figure 4.5: The effect of the Gabor filter on the CSI data (a) No movement (b) Movement.

4.4.5 Data Classification

The classification consists of training and testing. Each training sample contains a class label and several features. Classification is to determine the labels of the testing

4.4 Intrusion and Human Presence Detection System

samples according to their features, based on the models established using the training samples. For intrusion and human presence detection, two kinds of CSI samples need to be collected during training: (1) positive samples collected with human presence; (2) negative samples collected when vacancy as we discussed before . We use two classifiers to determine intrusion and human presence and the compare the results of each classifier to define the best one of them. Assume n is the number of training samples, l denotes the dimensionality of features. Each training sample consists of a pair (r_i, c_i) , where $r_i = (r_{i1}, r_{i2}, , r_{il})$ is a vector representing the features, i.e. CSI data after denoising technique and feature extractor, and $c_i \in (0,1)$ is the label assigned during training, with 1 representing the human presence and 0 representing vacancy. These labelled samples are used to establish the SVM [53], KNN [54] and CNN classifiers. We have used a convolutional neural network without any previous preprocessing and with just 105,419 trainable parameters. Assume (r, c) is a testing sample, with $r \in R^l$ as the CSI data, classification is to determine the value of c , i.e. to determine human presence or vacancy in the area of interest.

4.4.6 Results and Analysis

All the datasets have been split into a training set and a testing set with a ratio of 70% and 30%.

A- Evaluation Matrices

The system has been evaluated with a lot of matrices and techniques like accuracy, confusion matrix, and classification report.

1. Test set accuracy:

it's the ratio between the correctly predicted samples and the total tested samples. It's a good indicator during training to check the generalization of the network as the network has never seen the test set during training. it is defined as

$$\text{Test set accuracy} = \frac{\text{total number of correctly predicted samples}}{\text{total test set samples}} \quad (4.2)$$

2. Confusion Matrix:

The confusion matrix is used to provide a clear vision of the classification model results. on $X - axis$ there are the real classes and $Y - axis$ there are the predicted

4.4 Intrusion and Human Presence Detection System

classes. important matrices included in the confusion matrix: true positive samples (TP), true negative samples (TN), false-negative samples (FN), and false-positive samples (FP). These matrices are good indicators of the system's stability and tell how far the system's results are trusted.

3. Classification report:

The classification report provides important relations between the matrices of the confusion matrix. The classification report includes three important matrices:

- Precision:

It tells how many positive identifications were actually correct. Where it is defined as

$$Precision = \frac{TP}{TP + FP} \quad (4.3)$$

- Recall:

It tells how many actual positives were identified correctly. Where it is defined as

$$Recall = \frac{TP}{TP + FN} \quad (4.4)$$

- F1 Score:

Since precision and recall are in tension as changing the decision threshold will increase one of them and the other will decrease, we need another indicator that could be reliable to describe the classification performance F1 score is a weighted harmonic mean of precision and recall Where it is defined as

$$F1Score = \frac{2 * (Recall * Precision)}{Recall + Precision} \quad (4.5)$$

B- Task Results

We evaluated the system by SVM and KNN after using each denoising technique with PCA. The evaluation results are illustrated in Fig. 4.6, 4.7 and 4.8. This methods is able to achieve the detection accuracy up to 99.9% by DBSCAN with SVM and 99% with KNN, 99.3% by FFT with SVM and 98.3% with KNN and 99.4% by Butterworth low pass filter with SVM and 98.7% with KNN.

4.4 Intrusion and Human Presence Detection System

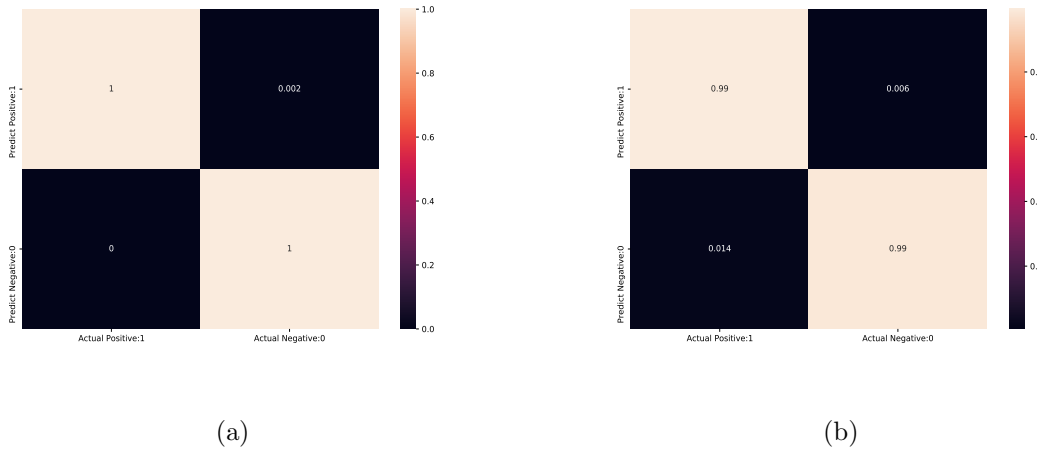


Figure 4.6: The confusion matrix for DBSCAN technique (a) SVM (b) KNN.

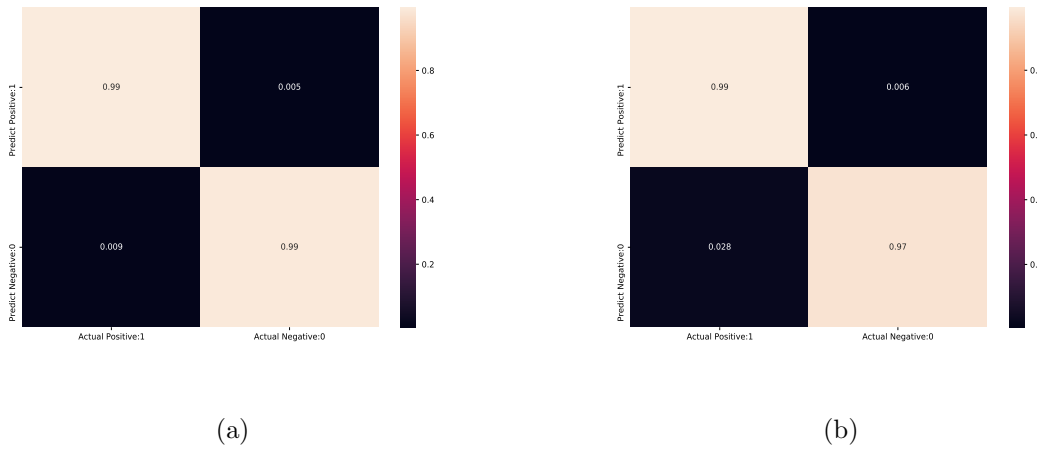


Figure 4.7: The confusion matrix for FFT technique (a) SVM (b) KNN.

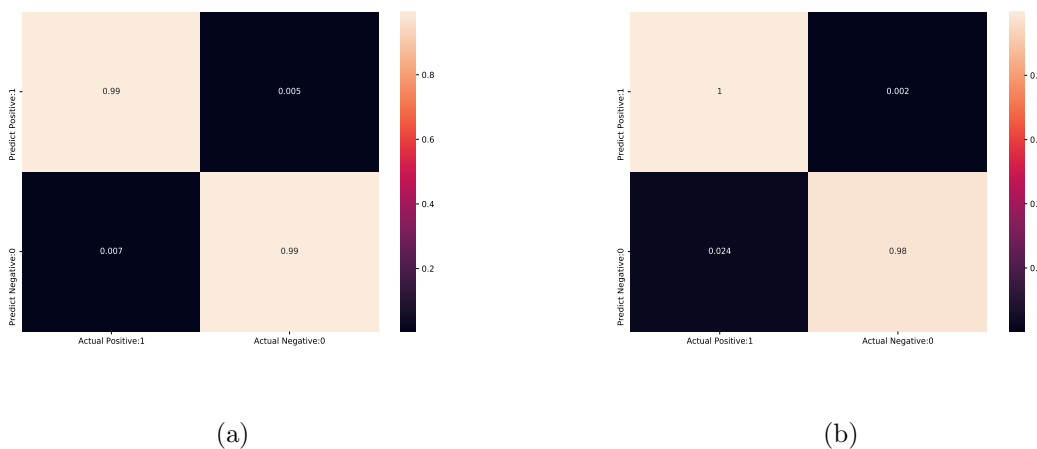


Figure 4.8: The confusion matrix for Butterworth low pass filter (a) SVM (b) KNN.

4.4 Intrusion and Human Presence Detection System

We also evaluated the system by using Gabor filter and CNN without any denoising technique. The results are illustrated in Fig. 4.9 and 4.10. Gabor filter is able to achieve accuracy up to 99.9% with SVM and 99.7% with KNN. Also, we got an accuracy of about 99.9% by CNN. Fig. 4.11 shows a comparison between the results of all the techniques used to detect intrusion and human presence.

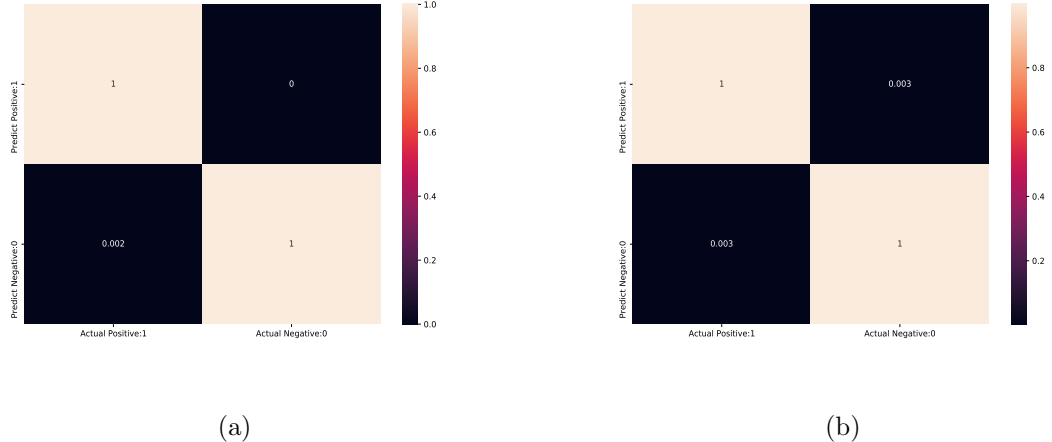


Figure 4.9: The confusion matrix for Gabor filter (a) SVM (b) KNN.

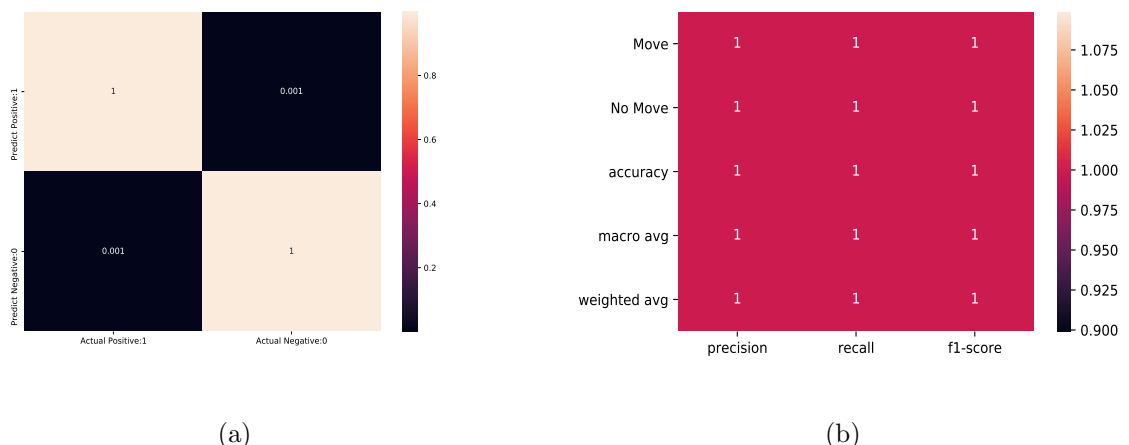


Figure 4.10: The system results by CNN(a) the confusion matrix (b) the classification report.

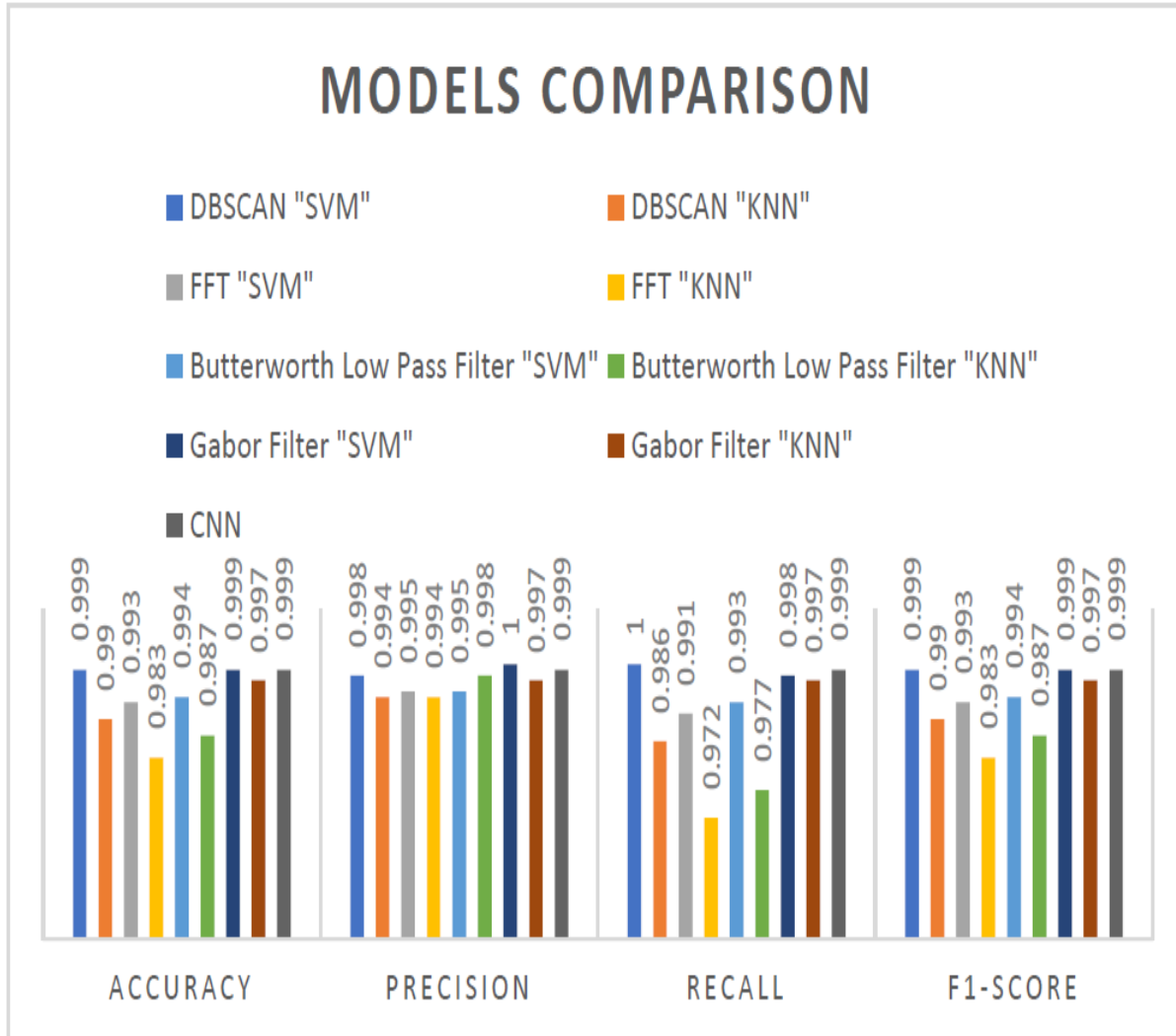


Figure 4.11: Comparison between the results of all models.

Chapter 5

GAIT RECOGNITION AND JOINT TASK

5.1 Introduction

Device-free gait-based identity identification has attracted much attention in recent years. It can recognize people in a specific area and identify them without requiring people to use any special electronic devices [58] [59]. The wireless-gait based identity identification techniques that take advantage of off-the-shelf infrastructure makes it more pervasive. There are many existing methods, which can achieve human recognition using gait, such as cameras or internal measurement units (IMU) [60].The limitations of the previous methods have prompted the researchers to search for new sensing solutions that are more suitable for indoor environments.

With the rapid development of wireless technologies in the past few years, the role of WiFi Radio Frequency (RF) signals has been extended from that of a sole communication medium to a non-intrusive environmental sensing tool. Advantage of the transmission characteristics of opportunistic WiFi signals in wireless channels is taken by the researches of WiFi-based sensing, such as Received Signal Strength Indication (RSSI) and Channel State Information (CSI), which are used in many applications such as, indoor localization, activity recognition, gesture recognition, human presence, vital signs, intrusion detection and so on. The detailed propagation of signals from the transmitter (TX) to receiver (RX) through multiple paths at the granularity of Orthogonal Frequency Division Multiplexing (OFDM) subcarriers is described by the CSI, both amplitude and phase information for

5.1 Introduction

each propagation path is contained by the CSI. By analyzing the changed signal paths and channel state on CSI impacted by moving targets, more accurate and robust intrusion detection and gait based identity recognition solutions can be achieved. More and more attention is gained by intrusion detection and gait identity recognition and they have great potential in many applications, such as border protection, smart homes, smart cars, elderly health care, etc...

WiFi gait recognition is based on the idea of when a person moves through wifi signals this person causes changes to amplitude and the phase that could be seen in the channel state information as in Fig. 5.1 and everyone has their own custom gait, where medical studies have shown that gait is a very complex biological process and is unique to each person [61] [62]. There are studies that also show that when we try to imitate someone else's gait our own gait works against us [63] [64]. These unique characteristics of gait make it ideal for user identification and authentication. Since gait causes custom changes and the WiFi signals are sensitive enough to detect these changes and deep learning helps us to classify them based on these changes.

WiFi intrusion detection and gait recognition have 6 main advantages over the other traditional techniques:

- Non-wearable and non-invasive devices:

Since the gait-modulated WiFi signals can be captured from a distance without user awareness and cooperation, they're non-intrusive and non-disruptive by nature, hence greatly increasing the usability of the authentication procedure.

- Low cost:

Having a low manufacturing cost led to the wide deployment of WiFi infrastructure, and with the prosperity of the Internet of Things (IoT) and the proliferation of WiFi-enabled smart devices, such as smart refrigerators, smart TVs, and smart thermostats, nearly everyone is surrounded, one way or another, by an invisible system of WiFi signals.

- Anti-spoofing:

Gait spoofing attacks don't work on gait recognition systems, so a person cannot imitate the walking style of someone else in order to gain illegitimate access and

advantages. Gait is potentially difficult to spoof since it's behavioral and encompasses the whole body as the existing research has shown [65]. What is even more counterintuitive is that as the spoofers devote more training efforts to gait mimicking, the results of the gait spoofing attacks become worse because our physiological habits work against us when we are trying to modify something as fundamental as the way we walk [66].

- Privacy issues:

WiFi sensing is non-intrusive and non-obtrusive by nature which leads to protecting the privacy of the users.

- Low power:

It is suitable for modern applications and IoT devices since they run on very low power.

- Robust against light conditions:

Being based on WiFi signals only makes WiFi sensing systems robust against light conditions.

Most systems that are based on solid hand-crafted analysis fail when dealing with a large dataset and huge numbers of users so we are going to build a system with a deep learning network. In this chapter, We propose BLAZE-WI, an intelligent, light weighted and privacy-friendly user identification and intrusion detection system that offers significantly higher accuracy and deals with joint tasks.

Our network is based on depth wise separable convolutional layers and we managed to classify a group of volunteers with a classification high accuracy, we are the first to build gait and intrusion schemes in the same system. In addition to this, we provide a comparison between multiple architectures and learning algorithms. This process works like any other deep learning-based process. In summary, our main contributions are as follows:

- Light-weighted network based on Blaze Blocks.
- Combining different schemes which are Intrusion and gait based human recognition in the same system.

- The results were achieved using commodity and commercial hardware without additional modification on the hardware.

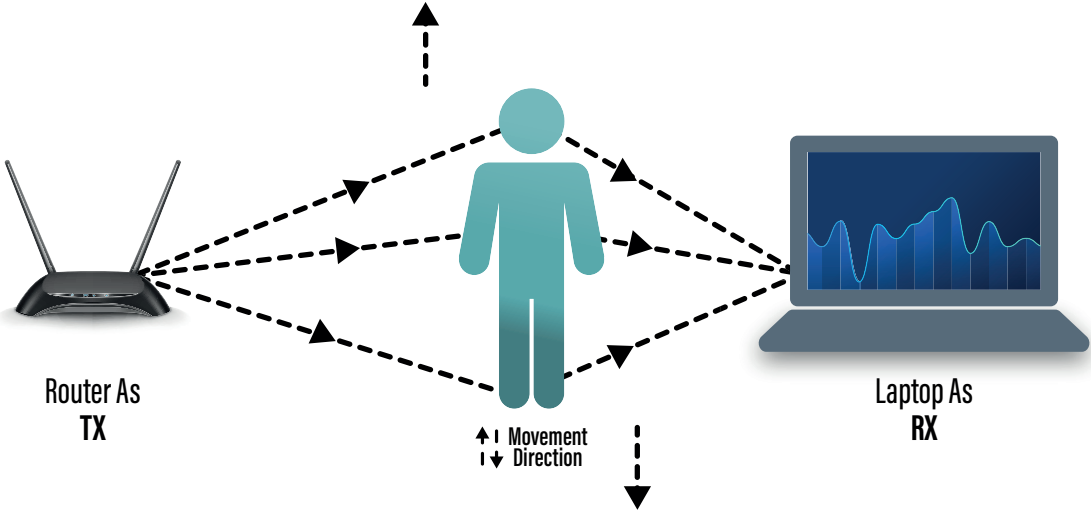


Figure 5.1: The general WiFi sensing system.

5.2 Related Work

5.2.1 Gait Recognition in the Old School

Johansson et al. [67] and Cutting et al. [68] conducted similar research in the 1970s and discovered that by simply viewing video pictures of the walker's prominent joints, viewers could identify the gender of the walker or even recognize the walker they were familiar with. Early human gait recognition systems were mostly relying on video or image sequences, based on these research foundations [69–72]. However, video-based methods always need subjects to walk perpendicular to the optical axis of cameras in order to obtain more gait information, [69] and they often have a number of other non-negligible drawbacks, such as LoS, light, and personal privacy. For gait recognition, some other advanced sensors were also used. Orr et al. [73] used floor force sensors to record the subjects' footstep force profiles, on which the footstep models were designed, and they were able to achieve a 93% gait recognition accuracy. Sprager et al. [74] and Primo et al. [75] presented collecting walking dynamics and recognising human gait using the built-in accelerometers of cell phones. A Gait, on the other hand, is not constrained by light or LoS conditions, and it does not require subjects to hold or wear any instruments

or deploy dense sensors.

5.2.2 Gait Recognition in the Modern School

Many applications [76–79], including gait recognition [80, 81]. have recently been developed using emerging Wi-Fi-based (mainly, CSI-based) sensing techniques. They proposed in [82], WiStep, a specialized step counting method that uses Discrete Wavelet Transform (DWT) and short-time energy calculation to reveal step patterns in CSI amplitudes, and it can be used to segment the CSI data of each step, i.e., gait cycle detection, for gait recognition. CSI gait features were used to extract time-domain and frequency-domain gait features. WiWho, WiFi-ID, and WifiU are three gait recognition systems proposed by Zeng et al. [81], Zhang et al. [83], and Wang et al. [80], respectively. WiWho concentrated on the CSI low frequency band 0.32 Hz, which involves a lot of interference caused by small movements and changes in the environment [82]. This prevents WiWho from working when the subject is more than 1 metre away from its transceivers' LoS route. In CSI measurements, WiFi-ID and WifiU focused on the frequency components of 2080 Hz. In WiFiID, gait features were extracted in different frequency bands using the Continuous Wavelet Transform (CWT) and RelieF feature selection algorithms, with the Sparse Approximation based Classification (SAC) [84] as the classifier. In WifiU, a synthetic CSI spectrogram was produced using Principal Component Analysis (PCA) and spectrogram enhancement techniques, from which a collection of 170 features was extracted, and the SVM classifier was then used for human identification. Based on WiWho, Chen et al. [85] added an acoustic sensor (a condenser microphone) as a complementary sensing module to detect gait cycles and developed Rapid, a multimodal human identification device that could provide a more reliable classification result than WiWho. From a group of 2 to 6 subjects, most of these systems could achieve an average human identification accuracy of around 92% to 80%. However, detecting gait cycles from CSI measurements is difficult because the changing patterns caused by walking are often hidden in the noise, [80] requiring the use of advanced signal processing techniques to fine-tune the data. Furthermore, hand-crafted gait features derived from gait cycles are constrained in their ability to classify complex walking patterns in various subjects.

5.3 Gait Recognition and Joint Task System (Blaze-WI System)

As shown in Fig. 5.2 a complete illustration of the Blaze-WI system design, which will be analysed through the following steps:

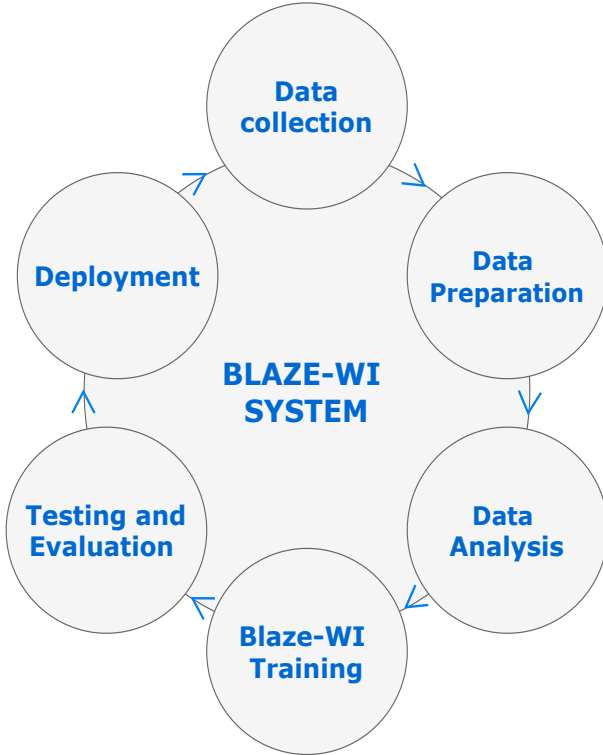


Figure 5.2: Blaze-WI system design.

5.3.1 Data and Topology

A- Hardware

A Dell Latitude E5400 laptop operating on Linux 14.04 LTS operating system has been used. It's equipped with Intel 5300 wireless NIC. A Linux 802.11n CSI Tool has been installed on the laptop [86]. A three-antenna access point (AP) operating at a 2.4 GHz band has been used.

B- Topology

As shown in Fig. 5.4, the test environment consisted of an empty corridor in the third floor of the main building of the faculty of engineering campus located in Suez Canal University in Ismailia. The environment is limited by the walls of the corridor and the horizontal distance between them is 210 cm and we refer to the horizontal axis as

5.3 Gait Recognition and Joint Task System (Blaze-WI System)

the x-axis. On the other hand, the vertical distance between the walls is 400 cm and we refer to the vertical axis as the y-axis. It's worth noting that the direction of gaiting is in the y-direction. The laptop and APs are fixed at the opposite sides of the corridor and horizontally facing each other. There are two end-points that are specified on the y-axis in the direction of gaiting.

C- CSI Data

As shown in Fig. 5.3, CSI contains meaningful data about the surrounding area which needs mining to extract them.

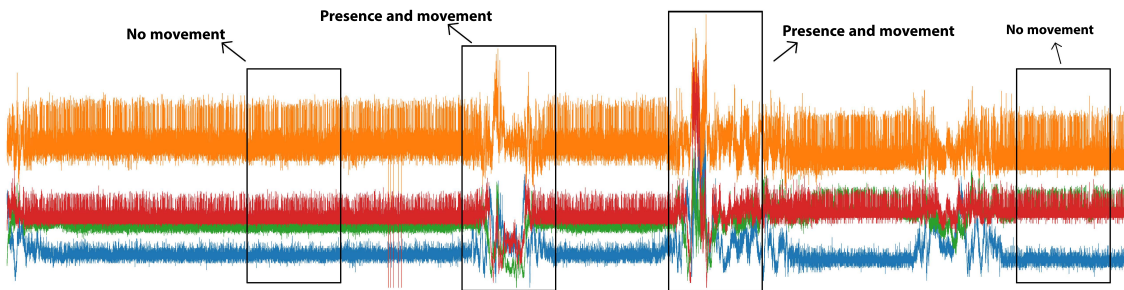


Figure 5.3: Presence and movement.

D- Data Collection

In this work, 8 participants (7 males and 1 female, aged between 20 to 26 years old) participated in the joint task dataset collection. Each participant is asked to walk within the horizontal distance between the two end-points in a straight line as shown in Fig. 5.4. As soon as the participant arrives at an end-point, they turn around and walk back to the other endpoint in a periodic motion. At the same time the laptop receives the packets from the access point then extracts the CSI measurements and saves it in a file named after the participant name. Six of the participants walked for 20 minutes while the other two walked only for 10 minutes with a total duration of 140 minutes (an alarm is being used to determine the end of the participant's walking duration). The sampling rate is 500Hz, the network input shape is [2500, 120] which means each sample is 5 seconds in duration. Each second the collected data shape is [500, 30, 2, 2] where 500 is the number of packets, 30 is the number of subcarriers, 2 is the number of TX antennas, and the last 2 is the number of RX antennas. Fig. 5.5 illustrates packet structure.

5.3 Gait Recognition and Joint Task System (Blaze-WI System)

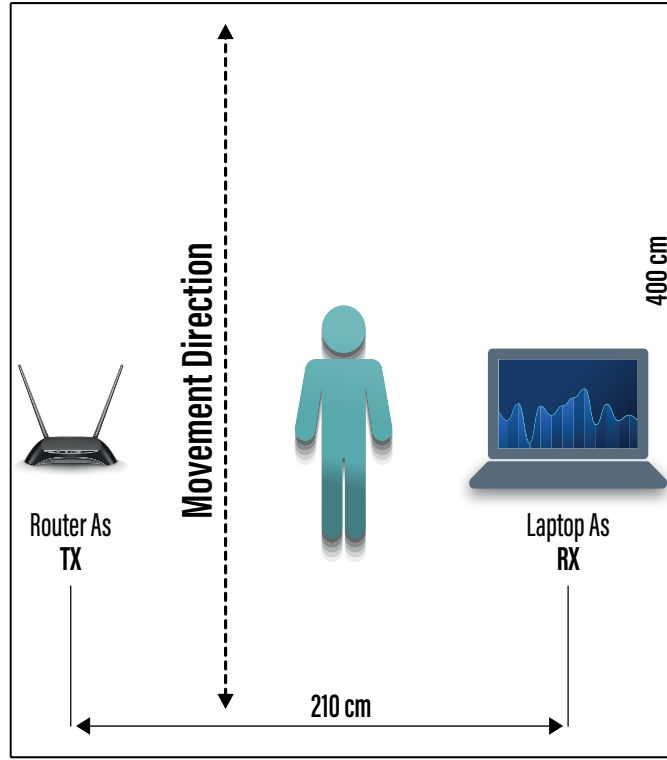


Figure 5.4: Configuration of the topology test.

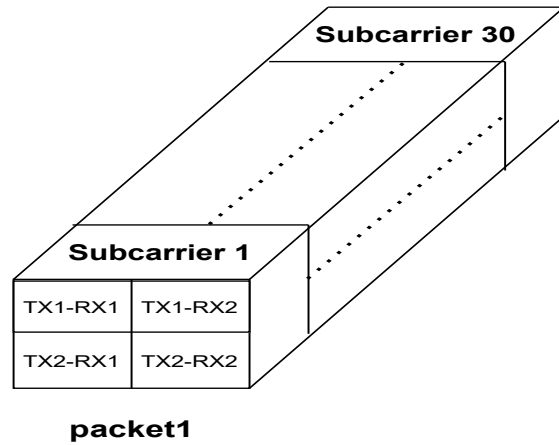


Figure 5.5: Packet explanation.

5.3.2 Network

A- Building Blocks

Blaze-Wi is inspired from Blaze-Face [87] network introduced by google and the building blocks are blaze-1D block and double-1D blaze block which are based on separable depthwise conv1D with kernel size of 5 as shown in Fig. 5.6. Blaze-Wi network considered

5.3 Gait Recognition and Joint Task System (Blaze-WI System)

as a function as follow.

$$Y = \text{Blaze-Wi}(CSI) \quad (5.1)$$

where CSI is 5 seconds of CSI collected data, Blaze-Wi is the network and Y is the result which then fed into the sigmoid function (5.2).

$$prob = \text{softmax}(Y) \quad (5.2)$$

where $prob$ is the probability distribution, softmax is the softmax function in (5.3) and Y is the output of the last layer in Blaze-Wi.

$$\sigma(\vec{z})_i = \frac{e^{z_i}}{\sum_{j=1}^K e^{z_j}} \quad (5.3)$$

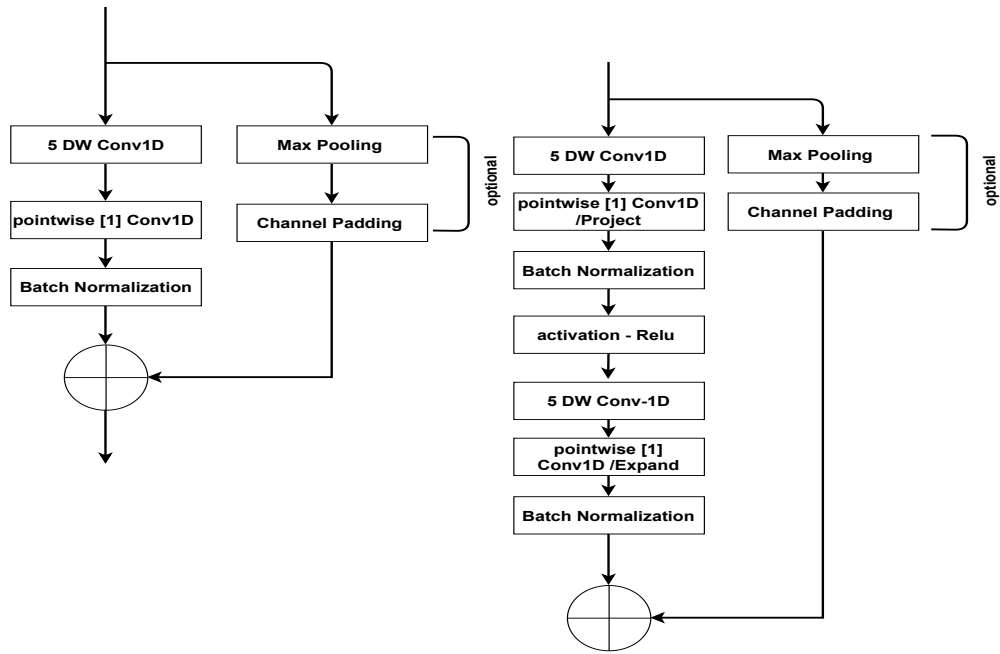


Figure 5.6: Blaze-1D block (left) and Double-1D blaze (right).

B- Separable Depth-Wise Convolution

Separable depthwise convolution (Fig. 5.7, Fig. 5.8) has become a very popular technique and is being used in many effective networks [Blaze-face, MobileNetV2, Xception] [87–89] and these techniques are used in our network as well. Separable depthwise convolution layer consists of two stages, the first one is the depthwise convolution layer which deals with each channel separately thus leading to reducing the operations required.

5.3 Gait Recognition and Joint Task System (Blaze-WI System)

Second, point wise convolution 1×1 convolution which is used to create the network features.

Convolution layer with a kernel size of $K * K$ and an input tensor $W * H * C_i$ is being used to produce an output of size $W_o * H_o * C_o$ so the computational power is $W_i H_i C_i C_o K * K$. While in the separable depthwise convolution the computation power is $W_i H_i C_i (C_o + K * K)$.

So thanks to separable depthwise convolution, a light-weighted and deep network have been managed to achieve. Skip connections allows us to avoid the vanishing gradient problem [90]. Also a batch normalization layer has been used with each building block which has a significant effect on the accuracy and number of epochs.

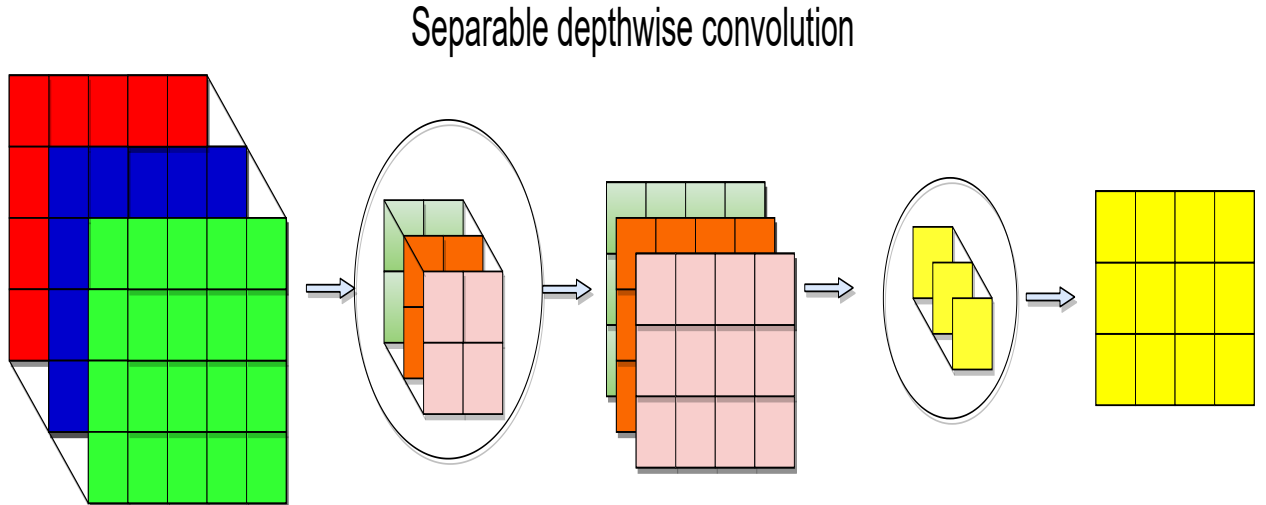


Figure 5.7: Types of convolution layers and the separable depthwise convolution.

5.3 Gait Recognition and Joint Task System (Blaze-WI System)

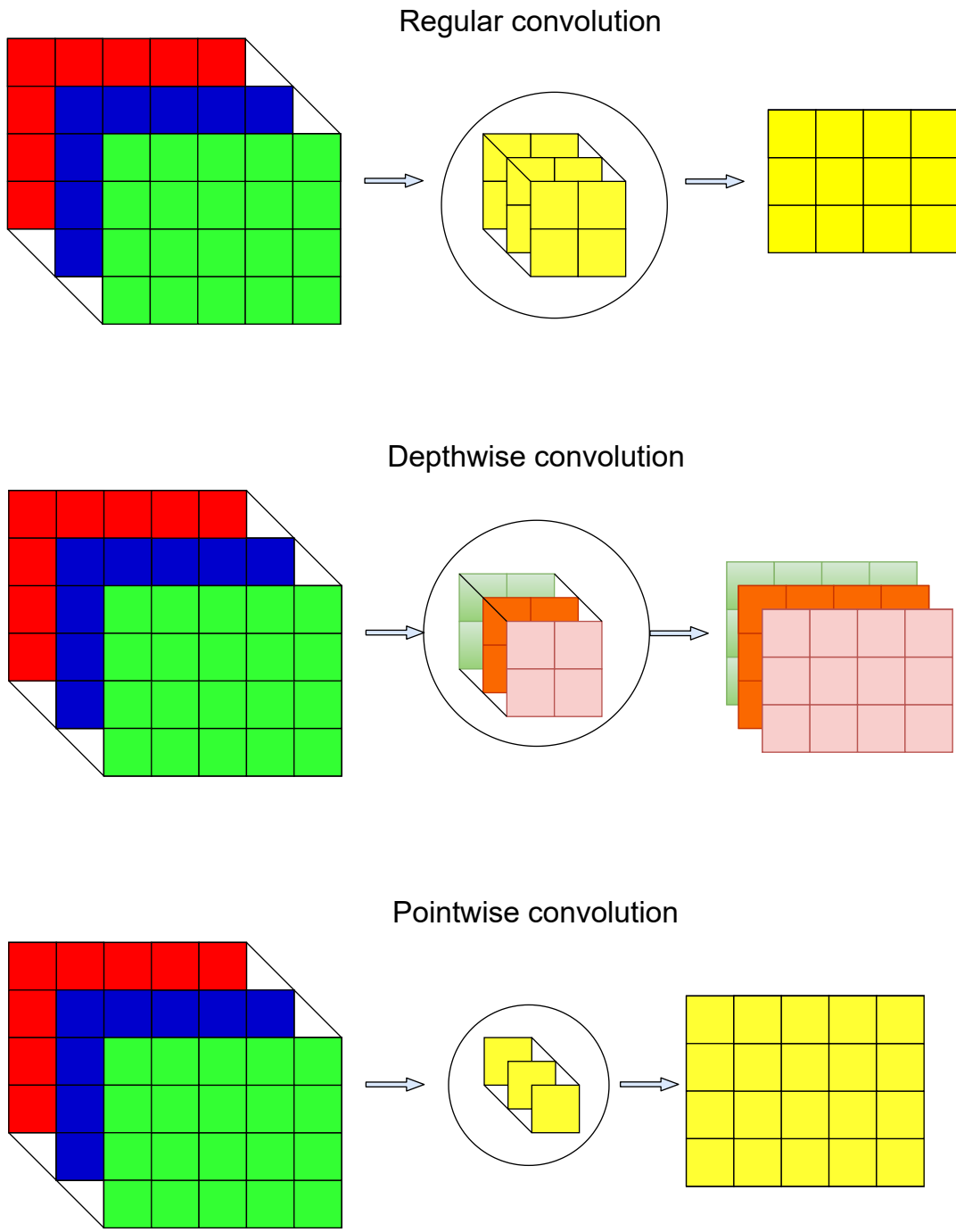


Figure 5.8: Types of convolution.

C- Full Network

The full network can be presented as in Table (5.1)

5.3 Gait Recognition and Joint Task System (Blaze-WI System)

Table 5.1: Full network

Layer/Block	Input Size	Kernel Size/Dense Num
normalization	2500*6	—
SeparableConv1D	-	$5 \times 24 \times 1$ (stride 2) $1 \times 24 \times 24$
Single Blaze-1D block	-	$5 \times 24 \times 1$ $1 \times 24 \times 24$
Single Blaze-1D block	-	$5 \times 48 \times 1$ (stride 2) $1 \times 48 \times 48$
Single Blaze-1D block	-	$5 \times 48 \times 1$ $1 \times 48 \times 48$
Single Blaze-1D block	-	$5 \times 48 \times 1$ $1 \times 48 \times 48$
Single Blaze-1D block	-	$5 \times 48 \times 1$ $1 \times 48 \times 48$
SeparableConv1D	-	$2 \times 48 \times 1$ $1 \times 48 \times 48$
double_blaze_block	-	$5 \times 48 \times 1$ (stride 2) $1 \times 48 \times 24$ $5 \times 24 \times 1$ $1 \times 24 \times 96$
double_blaze_block	-	$5 \times 48 \times 1$ $1 \times 48 \times 24$ $5 \times 24 \times 1$ $1 \times 24 \times 96$
double_blaze_block	-	$5 \times 48 \times 1$ $1 \times 48 \times 24$ $5 \times 24 \times 1$ $1 \times 24 \times 96$

5.3 Gait Recognition and Joint Task System (Blaze-WI System)

Table 5.1 continued from previous page

Layer/Block	Input Size	Kernel Size/Dense Num
double_blaze_block	-	$5 \times 48 \times 1$ (stride 2) $1 \times 48 \times 24$ $5 \times 24 \times 1$ $1 \times 24 \times 96$
double_blaze_block	-	$5 \times 48 \times 1$ $1 \times 48 \times 24$ $5 \times 24 \times 1$ $1 \times 24 \times 96$
double_blaze_block	-	$5 \times 48 \times 1$ $1 \times 48 \times 24$ $5 \times 24 \times 1$ $1 \times 24 \times 96$
SeparableConv1D	-	$2 \times 96 \times 1$ $1 \times 96 \times 96$
SeparableConv1D	-	$2 \times 96 \times 1$ $1 \times 96 \times 96$
SeparableConv1D	-	$2 \times 96 \times 1$ $1 \times 96 \times 96$
SeparableConv1D	-	$2 \times 96 \times 1$ $1 \times 96 \times 96$
flatten	-	1344
dense	-	64
classification	-	6 or 7 based on the task

5.3.3 Results and Analysis

All the datasets have been split into a training set and a testing set with the ratio of 80% and 20%. The test set was not provided to the model during training it's clearly new to the model to check the model generalization. No preprocessing has been done on the dataset except the normalization and let all the work to Blaze-Wi network.

Adam [91] optimizer has been used to optimize the network parameters with initial

5.3 Gait Recognition and Joint Task System (Blaze-WI System)

an initial learning rate of 0.001 .after each 150 epochs the best weights were picked and the learning rate decays by a factor of 5 .the total epochs were 600 epochs and the batch size was 64 .

A- Evaluation Matrices

The network has been evaluated with a lot of matrices and techniques like accuracy, confusion matrix, and classification report.Blaze-Wi achieved high results on these matrices on our collected dataset and WIDAR 3.0 [92] and that will be explained in the upcoming subsections.

B- Gait Task Results

1. Our Dataset

An accuracy of 97.3% has been achieved using the collected dataset as shown in the confusion matrix and the classification report in Fig. 5.9.

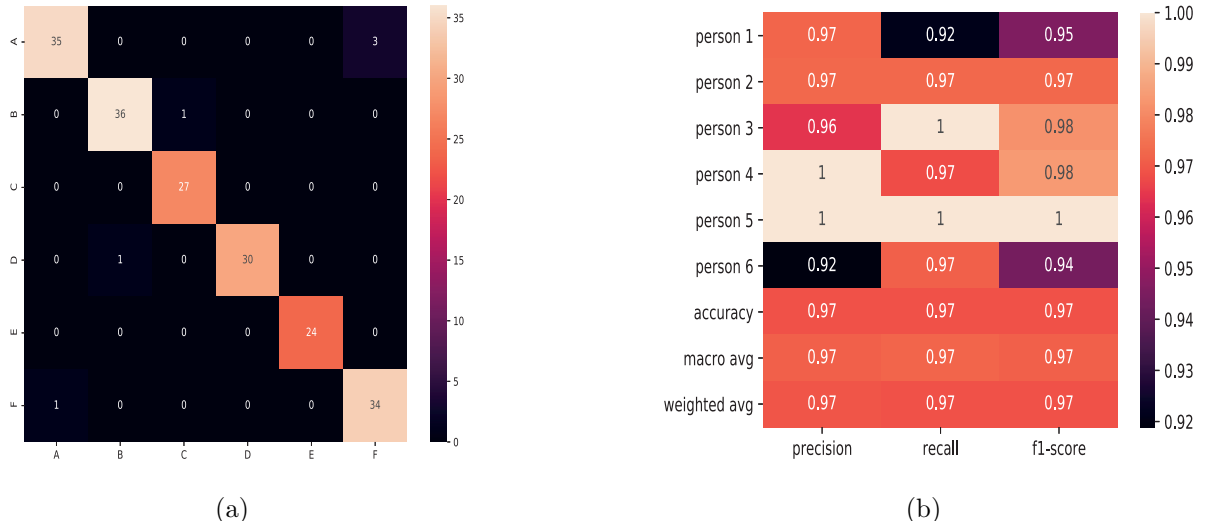


Figure 5.9: The gait-based identification system using our collected dataset for six volunteers (a) the confusion matrix, and (b) the classification report.

2. WIDAR 3.0

WIDAR 3.0 [92] has been used as it's a large dataset and 6 users have been chosen to train the network. Each user's data is about 2340 samples, our network has been trained with this dataset and managed to achieve a 99.27% accuracy with the test set Fig. 5.10.

5.3 Gait Recognition and Joint Task System (Blaze-WI System)

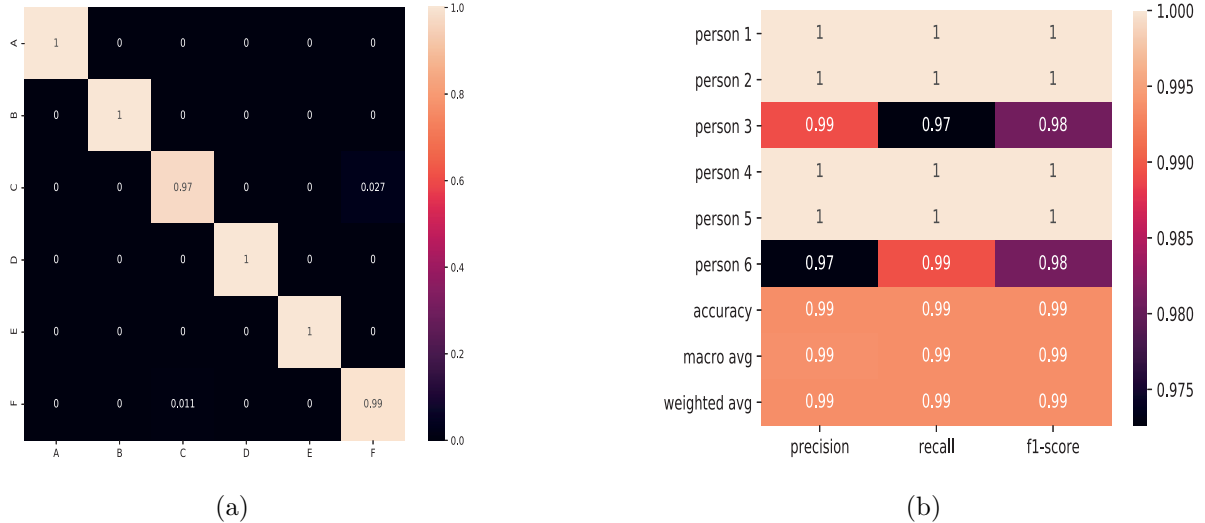


Figure 5.10: The gait-based identification on WIDAR 3.0 dataset for six volunteers (a) the confusion matrix, and (b) the classification report.

Our network shows significant results compared to GaitID [93] which got less than 92.5% with 6 users. Table (5.2) shows blaze-wi outstanding most of available systems with 6 users, taking into account differences in different datasets.

Table 5.2: Comparison with other systems with 6 users

System	Blaze-Wi	GaitID [94]	Blaze-Wi	Wihi [95]	Wii [96]	WiWho [97]	WiDIGR [98]
Classification accuracy	99.36	~90	97.3	96	91.5	80	78.28
Dataset	WIDAR 3.0 Data	WIDAR 3.0 Data	Our collected dataset	—	—	—	—

C- Joint Task Results

In the joint task gait-based identification and intrusion task on our dataset for six volunteers, an accuracy of 98.44% has been managed to achieve on the test set Fig. 5.11. These results show that identity recognition using gait and CSI is a powerful and promising technique. That should encourage us to build a suitable dataset similar to ImageNet in computer vision for example.

5.3 Gait Recognition and Joint Task System (Blaze-WI System)

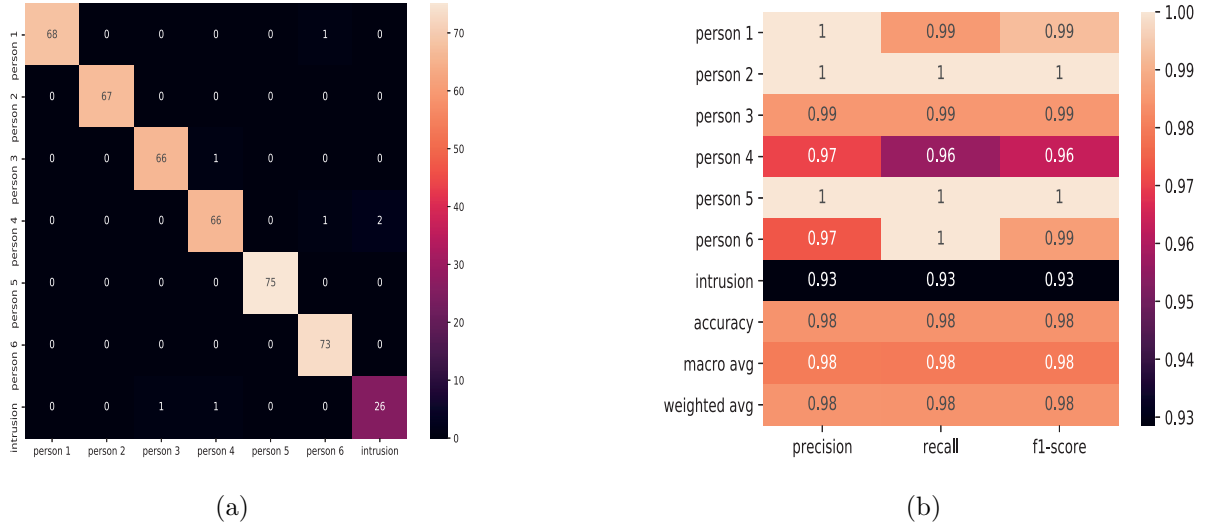


Figure 5.11: The joint task gait-based identification and intrusion task on our dataset for six volunteers (a) the confusion matrix, and (b) the classification report.

The experimental results demonstrate that BLAZE-WI can achieve 98.4% for the joint task, 97.3% for gait only, and with the WIDAR 3.0 dataset, it achieved 99.27% accuracy for a group of 6 persons as shown in Table 5.3.

Table 5.3: Comparison of Blaze-Wi with different datasets

Technique	Blaze-Wi WIDAR 3.0 data	Blaze-Wi Our dataset	Blaze-Wi Joint task
Accuracy	99.36	97.3	98.44
Precision	99	97	99
Recall	99	97	99
F1-score	99	97	99

Chapter 6

LOCALIZATION BASED ON RSSI

6.1 Introduction

Sensor based localization is a challenging task, since it is necessary to find an accurate solution that has a low cost and low energy consumption. A simple and intuitive solution to locate nodes in a wireless sensor network would be to equip them with GPS devices. However, this solution is more suitable for outdoor environments, since its use in indoor environments is quite limited. An alternative solution is to exploit internodes communications and metrics of radio-frequency transmissions between sensors. However, the most important issue remains in choosing what metrics to use, Common considered metrics include Time of Arrival (ToA), Time Difference of Arrival (TDoA), Angle of Arrival (AoA), and Received Signal Strength Indicators (RSSI).

RSSI-based techniques are the most attractive ones since received signal strength information is already available in many existing technologies such as Zigbee, Bluetooth, and WiFi. Therefore, no additional hardware is needed, making this solution the most promising one with respect to cost and simplicity. But in the actual applications, the distance measurement based on RSSI is influenced by reflection, multipath, antenna gain, and so forth, and large positioning error is caused. Therefore, instead of using RSSI to estimate the distances then find the target's position, we use RSSI with the fingerprinting technique to estimate the target's position without having to estimate the distances, this method can reduce the impact of environmental factors.

The operation of fingerprinting is done by three steps: first, the area which we want to make localization at will be divided into numbers of grids, and we collect the RSSI from

all access points (APs) in each grid. Then, we store all the RSSI values into a fingerprint database. Finally, the localization results are obtained through the similarity matching between the real-time RSSI value vector of mobile devices and fingerprint database in actual positioning.

6.2 Related Work

6.2.1 Wi-Fi Indoor Localization Using Crowdsourcing

In the beginning, crowdsourcing participants contributed location-labeled RSS samples for radio-map establishment with indoor electronic maps [100, 102]. Then Mirowski et al. [103] deployed a number of 2-D code labels in their experimental area for users to scan and obtain location information. Wu et al. [104] recorded numerous trajectories of crowdsourcing participants and then matched the trajectories with RSS data using multidimensional scaling (MDS). In [105], a survey-free algorithm called Chameleon was proposed to filter out altered APs with crowdsourcing data. Wang et al. [106] proposed an indoor sub-area localization method that constructed sub-area radio-map with crowdsourcing data and related them to indoor layouts. Jiang et al. [101] proposed a probabilistic radio-map construction for crowdsourcing-based fingerprinting method. The method required a large number of RSS samples. Unlike above-mentioned literatures that focused on crowdsourcing-based fingerprinting localization, Zhuang et al. [107] estimated PM parameters with crowdsourcing data for AP localization. Then localization coordinates were computed with trilateration localization. The system required a certain number of crowdsourcing data collected from the participants' daily life. By contrast, our proposed crowdsourcing-based PM localization method only needs crowdsourcing data from a few CPs, which can be easily collected in a short time.

6.2.2 Camera-Based Indoor Localization

So far, many camera-based localization systems have been proposed. With 2-D image physical properties, locations and heights of people were estimated by a constrained optimization process in multiple calibrated camera networks [108]. Liu et al. [109] first focused on the localization-oriented coverage of the camera network and then formulated the localization problem using Bayesian estimation to compute a needed camera den-

sity. Liu et al. [110] proposed a location-constrained maximum a posteriori algorithm for camera-based localization through incorporating camera parameters and location information. Pflugfelder and Bischof [111] formulated camera-based localization and trajectory reconstruction as an optimization problem that could be solved by singular value decomposition (SVD). Also, Lin et al. [112] presented a series of image transforms based on the vanishing point of vertical lines, which improved their probabilistic occupancy map (POM)-based localization method. Compared with the camera-based indoor localization methods above, our method is capable of covering an area and locating people with only one panoramic camera.

6.2.3 Indoor Localization Using Multi-Source Heterogeneous Data

To offer accurate location information for users, people have tried to exploit multi-source heterogeneous data for indoor localization. The expressions of the Cramer-Rao lower bound (CRLB) were given using heterogeneous information under NLOS conditions, which showed that the condition of localizability could be almost always fulfilled for connected range bearing networks [113]. Nguyen et al. [99] presented a vision-enhanced wireless localization method that successfully integrated vision information and TOA measurements of UWB for cooperative localization in harsh indoor environments. In [114], Denis et al. emulated a multi-mode terminal based on ZigBee and orthogonal frequency division multiplexing (OFDM). Their experimental results proved that more accurate location of the terminal could be estimated through cooperation, data fusion and node detection. Liu et al. [115] proposed a peer assisted localization approach using RSS and acoustic signals. The approach could reduce the maximum error to 2m. Chen et al. [116] presented a smartphone inertial sensor-based localization and tracking approach using Wi-Fi and iBeacon. The localization accuracy of the approach was 1.39m. Unlike [116], using Wi-Fi and FM wireless fingerprints, a system proposed in [117] only had a localization accuracy of room level. Therefore, although various localization systems using heterogeneous data have been developed, to the best of our knowledge, no indoor localization system using Wi-Fi, panoramic camera and map information has been proposed so far.

6.3 Fingerprinting Method

In the course of wireless localization based on RSSI fingerprint feature vector, the RSSI values received from all of the wireless APs make up the fingerprint feature vectors of the location grids, and the fingerprint database is established. Then the real-time RSSI value vector received can be identified for fingerprint positioning. Its positioning process is divided into two stages, which are the establishment of fingerprint database and real-time positioning, and shown in Fig. 6.1.

In the operation of RSSI fingerprint wireless localization based on feature vector, first, a lot of Wi-Fi signal devices are arranged (typically wireless APs), and the number of APs is in correspondence with the dimensions of the vector, here represented by k . Then the localization area is divided into a number of grids, here represented by $G_{i,j}$ ($i < m, j < n$). Finally, the mobile device (MU) can be located via grid matching between real-time RSSI value and fingerprint database [100].

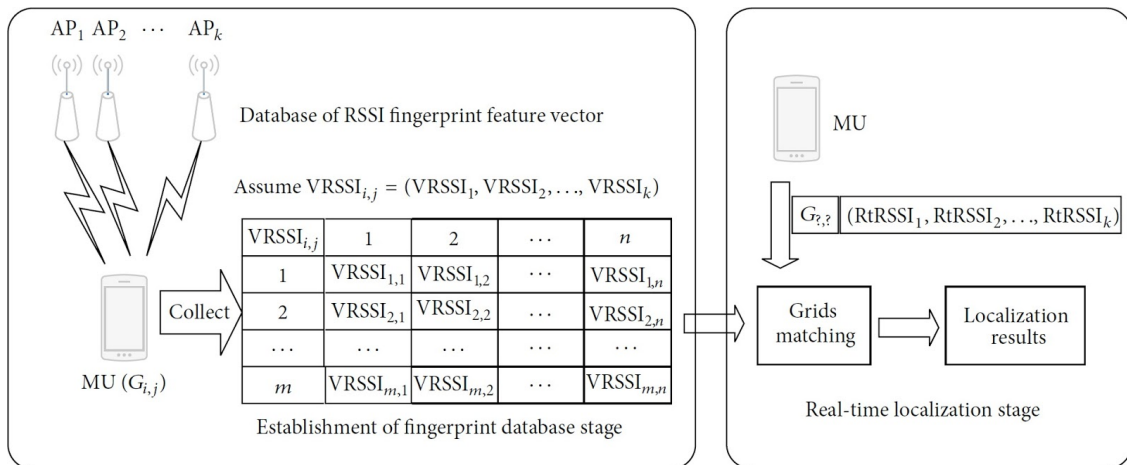


Figure 6.1: Framework of Wi-Fi localization based on RSSI fingerprint.

Now we will introduce the operations of RSSI fingerprint localization separately in the following.

6.3.1 Data Collection Points Arrangement

As shown in Fig. 6.2, the location area is divided into closely linked grids, and the grids can be sized and shaped. The size of the grid represents spatial positioning accuracy. All grids are numbered from southwest to northeast orderly, and there are a lot of wireless

6.3 Fingerprinting Method

signal devices in the targeted area, ranked by $AP_1, AP_2, AP_3, \dots, AP_k$.

In the course of RSSI collection, all the RSSI values from APs in each grid will be collected and also the corresponding MAC address will be recorded. Typically, the larger vector dimensions of k , the higher the difference between different vectors. Enough wireless APs should be laid in the location area to improve the wireless Wi-Fi positioning accuracy, but it will make the RSSI data much bigger. For example, a location area is $100 \times 80\text{m}$, mesh size is $2 \times 2\text{m}$, and the number of the wireless APs is 20, then the recorded number of RSSI values to be stored is $100 \times 80 \times 20 / (2 \times 2) = 40000$.

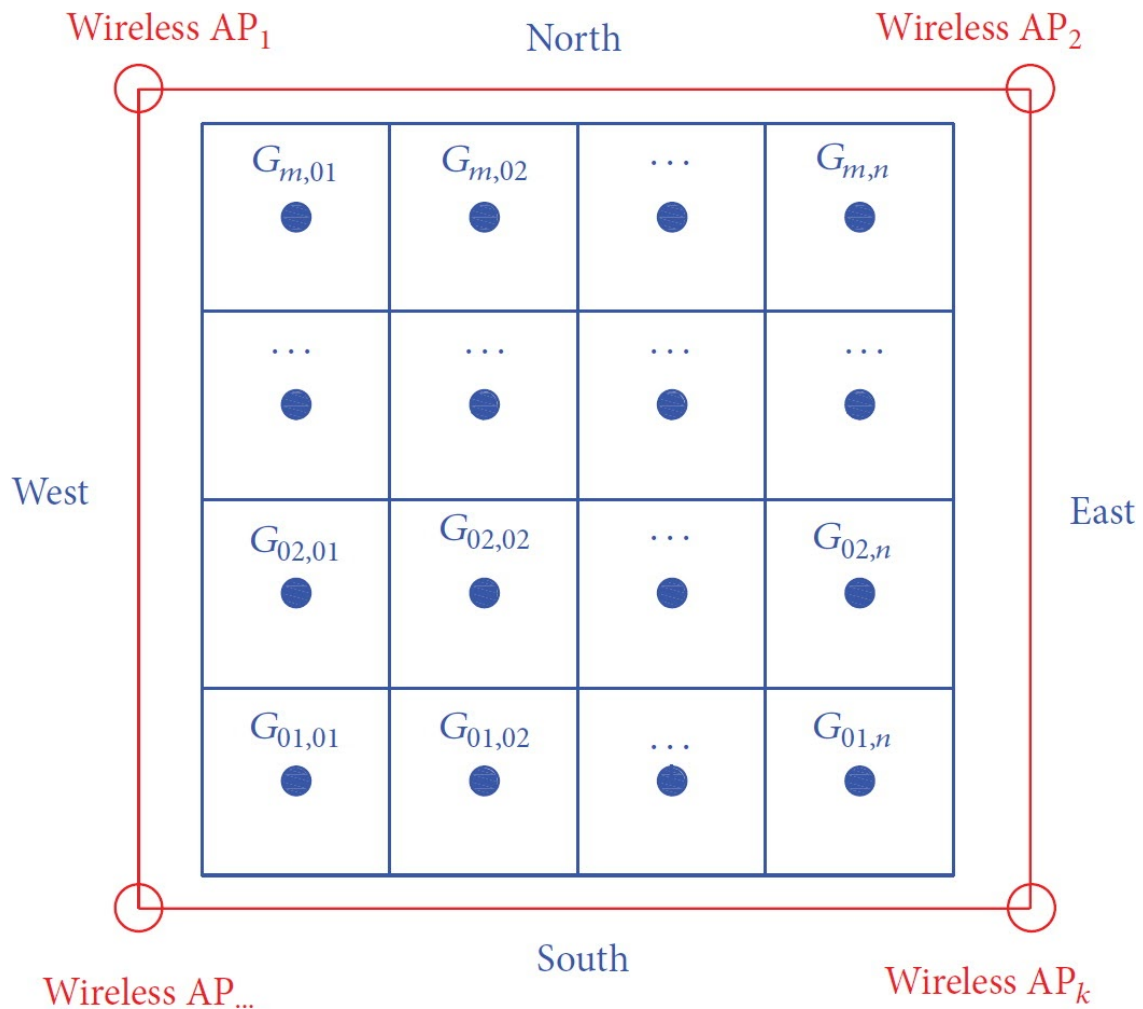


Figure 6.2: Schematic diagram of grid data collection in localization area.

6.3.2 RSSI Fingerprint Data Organization

Each time we do a localization operation, there is a large amount of RSSI fingerprint data that needs to be read. So, we need to use more efficient way of data organization in terms of matching algorithm characteristics on RSSI feature vectors. To improve the flexibility of data management of all APs, each AP data is stored in a separate table, and all tables have the same structure (number of tables equal the number of the APs).

Table 6.1: The structure of RSSI data.

MACid	C01 (text)	C02 (text)	...	Cn (text)
Record 01	...	Record 01	...	Record 01
:	:	:	:	:
Record m	...	Record m	...	Record m

In Table 6.1, m corresponds to the row value, and n corresponds to column value. The primary key of each record is the MACid, and C01,C02, \dots ,C correspond to the column of RSSI data table. Therefore, Record 01, \dots , and Record m correspond to collection records of RSSI value. Names of RSSI data table are identified by the APs' MAC address. We should make sure that the data table names are unique, and the data table element values are in correspondence with the collected values of RSSI in grids. In practical applications, the number of wireless APs may appear as changes with equipment damage, updates, and so forth; to this end, the fingerprint database must be adjusted. Therefore, only the changed RSSI data tables need to be updated, and the modification of the database can be accomplished easily, and the design of the database has good flexibility. In the course of localization, the RSSI data from all the APs must be queried and read, and its process from data query to build a fingerprint feature vector is shown in Fig. 6.3. In light of the given row and column of the grid ranked by $G_{i,j}$, the RSSI data of $G_{i,j}$ from all the tables are queried, and the corresponding k-dimensional feature vector of $G_{i,j}$ can be built. So, the k-dimensional feature vector can be exported for real-time location matching.

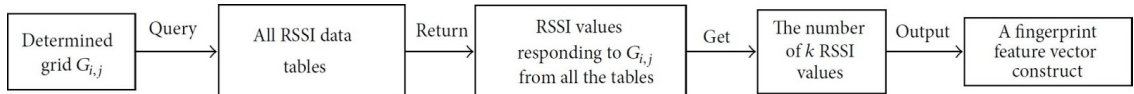


Figure 6.3: The process of RSSI data query and fingerprint feature vector construct.

6.4 Localization System

As shown in Fig. 6.4 a complete illustration of the localization system design, which will be analysed through the following steps:

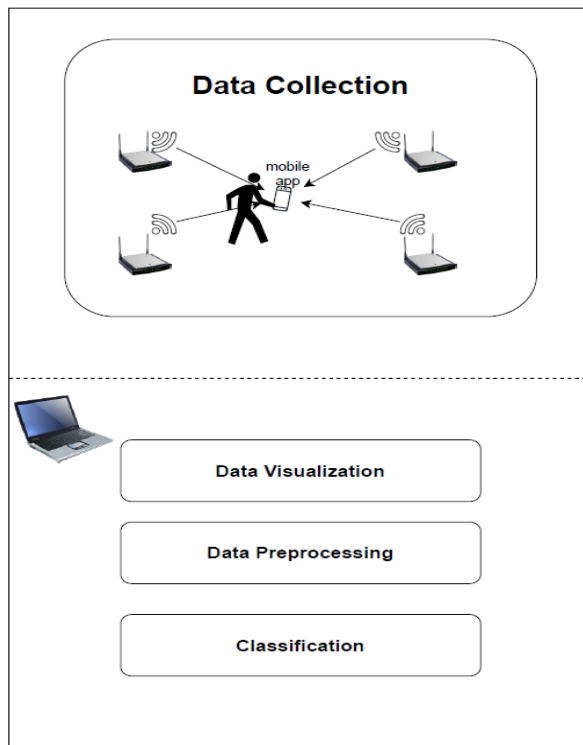


Figure 6.4: Localization system design.

6.4.1 Data Collection

A- Hardware

A Lenovo Vibe-C A2020 phone is equipped with a mobile application - described later – is used to record the fingerprint of the grid and 4 APs are used to transmit the WiFi signal.

B- Topology

Topology is specified as a small hall, its dimensions shown in Fig. 6.5. The hall is divided into grids which are called the fingerprint method described later and the APs are configured as shown in Fig. 6.5.

C- Fingerprint Method Implementation

The hall is divided into grids. 1 m is the distance between the grid and the next one in the y-axis and the x-axis. The volunteer stopped on each grid for 6 minutes holding the phone fixed at height 1.7m. The phone runs the mobile application “RSSI Collector” which records the RSSI for each AP at the same time and saves it to the phone storage.

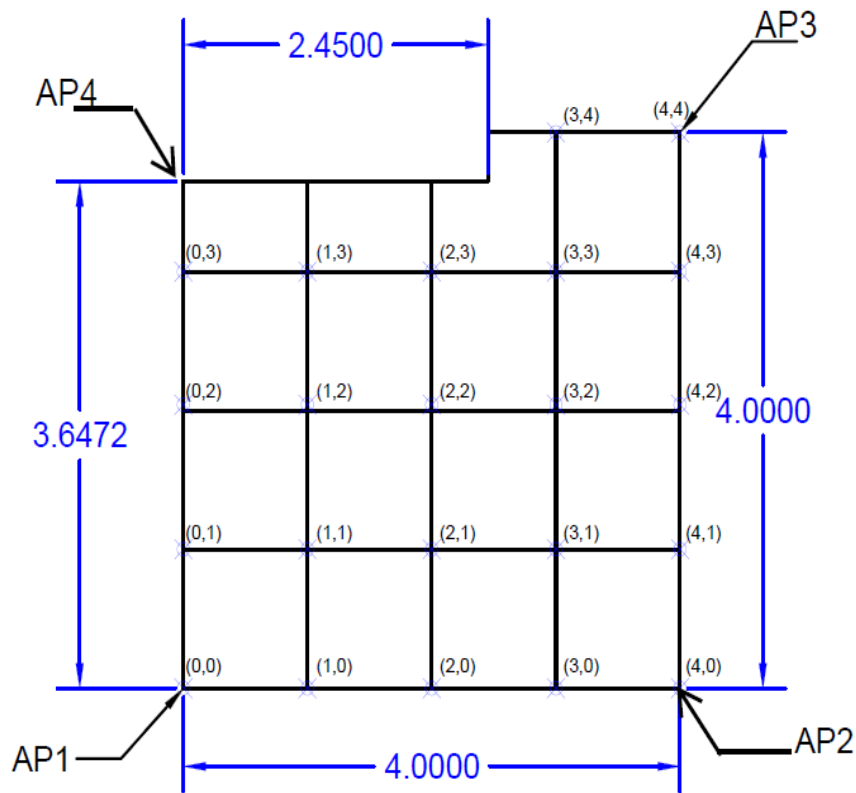


Figure 6.5: Topology.

6.4.2 Mobile Application

To build our own RSSI fingerprint database, we made an Android app using Flutter to collect RSSI values. We used the Flutter wifi package to be able to connect with wifi APs and collect RSSI. We also used the Flutter CSV package to build CSV files with

6.4 Localization System

the collected RSSI values, which is the output of the application. The application is consisting of two main screens as shown in Fig. 6.6 and their details as follows:

A- 1st Screen

In this screen we ask the user to enter the project name which may be the name of the area at which we want to make localization.

B- 2nd Screen

In this screen we ask the user to enter three things. Firstly, the number of samples that he wants to collect in the scan. Secondly, the wifi APs SSID which he wants to collect data from, and he has limits to three APs to choose and enter their SSID. Finally, the area name (grid name) which he will start to collect data in. Then the user will press the “Scan” button to start to collect data with a sampling rate of 1 sample per second. As we said before, the output will be a CSV file and its name will be the same name of area (grid) name which the user has entered, and this file can be found in the mobile internal storage in a folder that has the same name of the project name which the user has entered in the application first screen.

6.4 Localization System



Figure 6.6: Mobile application screens (a) 1st Screen, (b) and (c) 2nd Screen.

6.4.3 Data Visualization

The mobile application records the RSS with refresh rate 1 sample/sec. For each grid, RSS is being recorded for 6 minutes which results in 360 samples per AP for each of 22 grids. The shape of data is 7920 x 4 which results in data size 31680. Graphs in Fig. 6.7 shows the RSS in dB plotted relative to samples for each grid.

6.4 Localization System

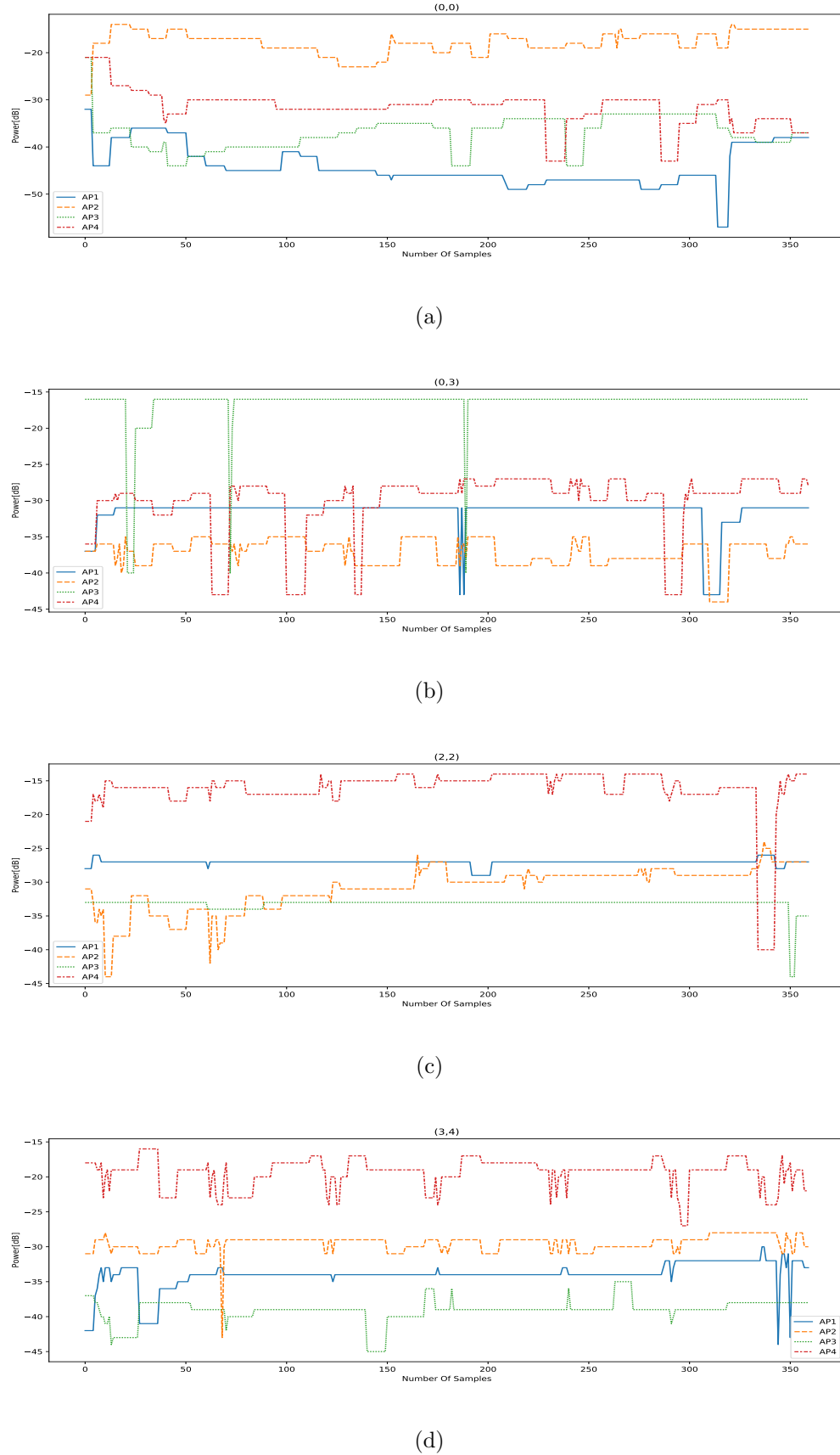


Figure 6.7: Data visualization graphs (a) RSS recorded for point (0,0), (b) RSS recorded for point (0,3), (c) RSS recorded for point (2,2), (d) RSS recorded for point (3,4).

6.5 Results and Discussion

Data is labeled and shuffled, and a normalization has been applied on data. ML classification models has been used and trained to classify grids data. Support vector machine (SVM) and kNN have been used and the results for SVM came as following: rbf SVM test is 97.811%, poly SVM test is 96.801%. for kNN the results came as 99.66% for training and 99.306% for testing. Fig. 6.8 shows the comparison between the accuracies for the models. Fig.6.9 shows the comparison between the three models' confusion matrix.

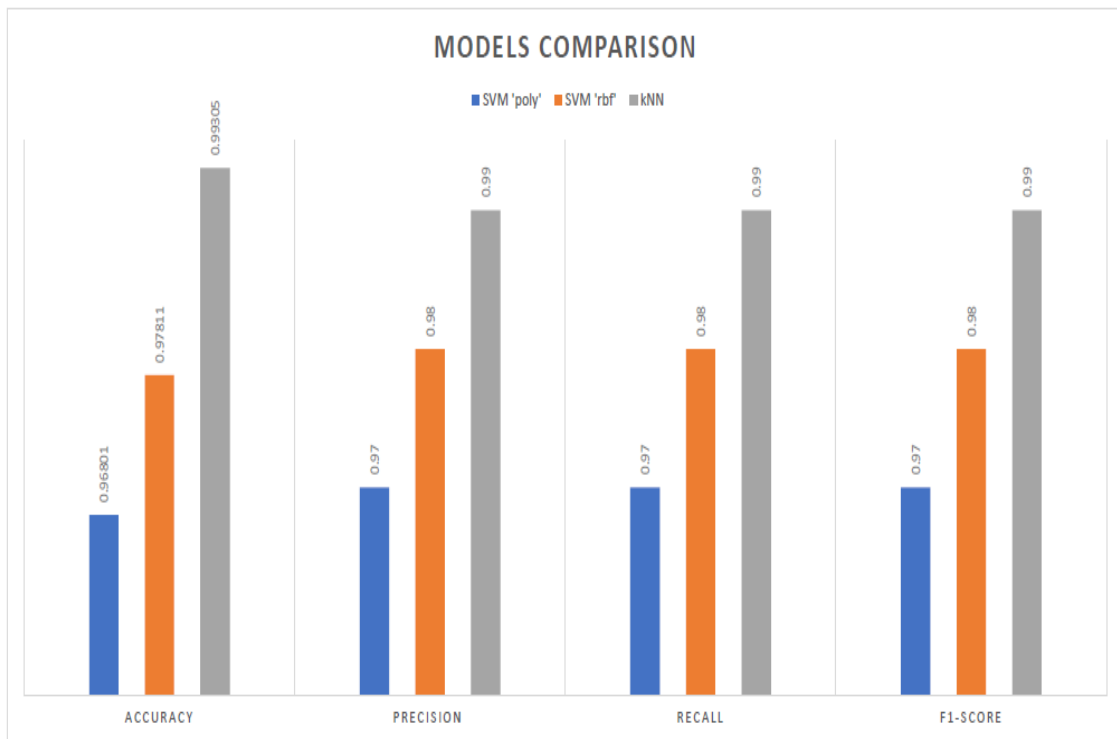


Figure 6.8: Comparison between three models accuracies.

6.6 Future Vision and Applications

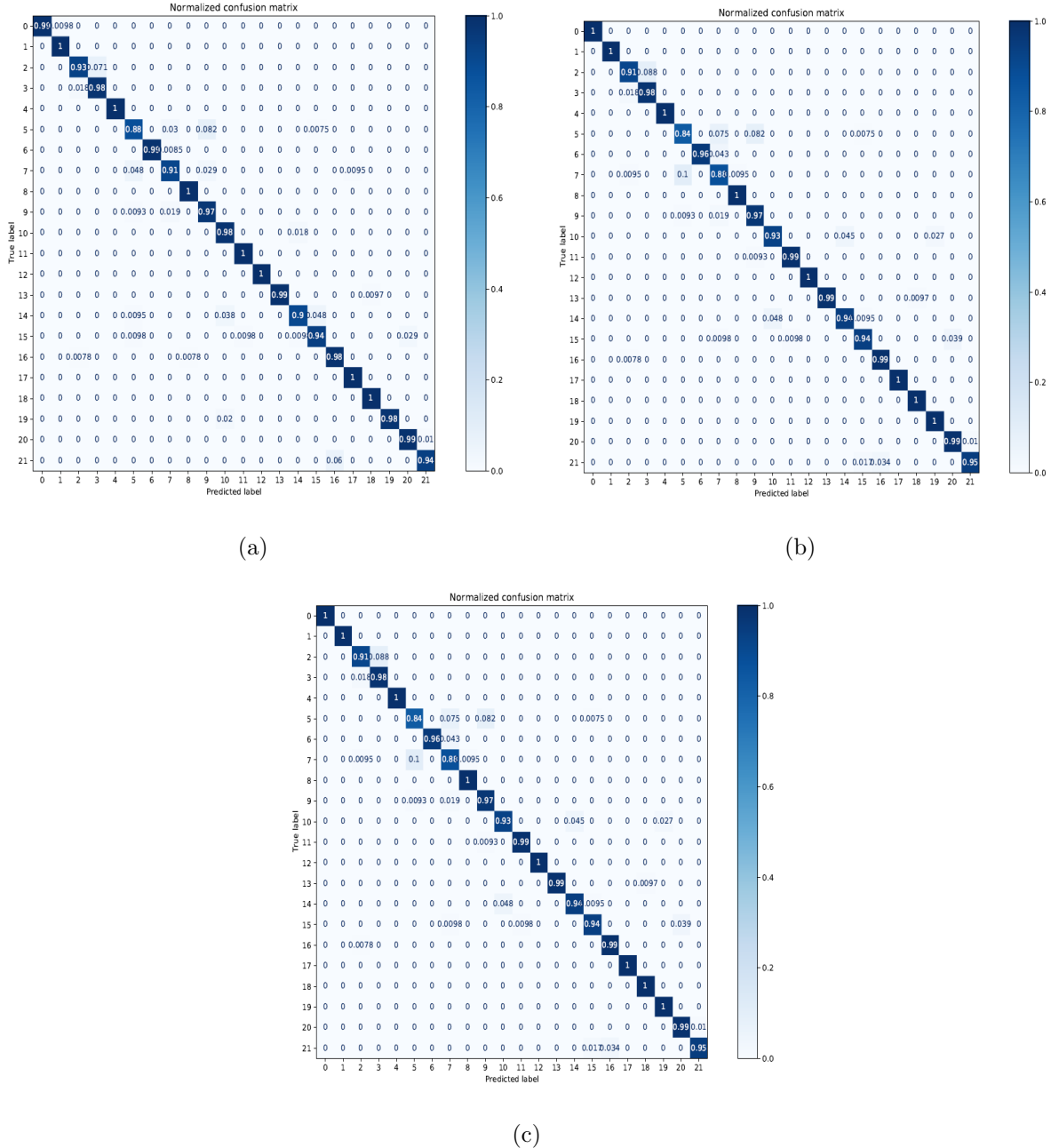


Figure 6.9: Confusion matrix (a) SVM "rbf", (b) SVM "poly", (c) kNN .

6.6 Future Vision and Applications

The localization based on WiFi sensing (RSS) system is not only a passing project, but rather an introduction to powerful applications that serve all fields, levels and disciplines. Our future vision is looking forward to extracting very powerful applications that can help lots of establishments to achieve their missions in the best possible way. Our perceptions has come as follows:

6.6.1 Retail

We can build a shopping mall navigation system and indoor store mapping system that can provides:

1. Indoor navigation and product search:

We help retailers improve customer experience via customer location mall mapping software, which provides navigation shopping mall and product search inside stores. Visitors may use a mobile grocery store navigation app to plan their routes on the basis of purchase list, search information about brands and select departments to go. It helps to increase customer engagement and loyalty that leads to additional revenues.

2. Customer traffic analytics and visitor site tracker:

Customer data enables marketers to understand the cross-channel behavior of visitors in shopping centers who become customers. Retailers need an accurate analytics tool that can clearly articulate the customer journey within a store that can in turn be used to personalize the shopping experience.

3. Marketing communication:

Using our system, marketers get an opportunity to deliver relevant, highly engaging content to consumers through a mobile shopping mall navigation app. It is possible to send instant greetings to the customers and get their attention with information about current special offers, sales while being close to the proximity hot spots.

4. Staff efficiency tracking.

6.6.2 Transportation

Our system can also play a very important role in transportation hubs. So the system can provide:

1. Passengers wayfinding in airport and train stations:

It's hard to imagine our lives without location based services. In such situations indoor navigation comes in handy. Our technologies allow us to build great solutions for indoor navigation for airports and railways. We detect a passenger's position and suggest the best wayfinding inside a building.

2. People flows tracking:

Flows of people vary significantly during the day with peaks in different times and destination points: in the airport gates, information points, baggage claim area, railway platforms and other places. A large congestion of people in the same location may cause the formation of bottlenecks. Which is, in turn, may lead to interrupted operations and cause risks for people's safety. Optimization of people flows is a big challenge. Especially in light of novel covid-19 current conditions.

6.6.3 Warehousing and Logistics

Our project also can help in a Real-time tracking system for warehouses to keep control on the assets, vehicles and staff. So the system can provide:

- 1. Warehouse Asset Tracking System.**
- 2. Staff Navigation and scheduling.**

6.6.4 Manufacturing

Our system can also give a comprehensive powerful navigation and assets tracking system for safety improvement and manufacturing efficiency enhancement (e.g. real-time motion monitoring, assets and vehicles tracking and staff tracking).

And also have many others (e.g. Healthcare, Sport, ...etc).

Chapter 7

CONCLUSIONS

7.1 Conclusions

OFDM and MIMO make it possible to access fine-grained physical channel frequency response of multiple links, thus trigger the use of CSI to achieve more accurate device-free for more approaches such as intrusion detection, gait recognition, indoor localization and so on. So, we present a CSI-based device-free Intrusion and human presence detection system, user identification system based on the gait biometrics extracted from WiFi signals, and a joint system combining the intrusion detection and user identification systems in one system. In an intrusion detection system, we apply SVM, KNN and CNN to solve the presence detection problem through classification. We have applied more than one denoising technique such as DBSCAN, FFT and Butter worth low pass filter on CSI data to reduce the noise and we also used both PCA and Gabor filter to extract the features and reduce dimensionality. Evaluations of this system prove the effectiveness of the algorithm, achieving the intrusion and human presence detection accuracy up to 99.9% by DBSCAN with SVM and 99% with KNN, 99.3% by FFT with SVM and 98.3% with KNN and 99.4% by Butterworth low pass filter with SVM and 98.7% with KNN. We also evaluated the system by using Gabor filter and CNN without any denoising technique. Gabor filter is able to achieve accuracy up to 99.9% with SVM and 99.7% with KNN. Also, we got an accuracy of about 99.9% by CNN.

For the gait recognition system and joint task system, The deep learning side has been focused on to extract the necessary features for the model except for the hand-crafted feature extraction and traditional algorithms. Our network, Blaze-Wi, which is inspired

by Google's network BLaze-Face has only 210 thousand parameters which allows it to perform real-time predictions. The hyperparameters have been tuned to achieve ideal results. As a result, for a group of 6 persons, the network managed to achieve a 98.44% accuracy for the joint task, 97.3% for gait only and with the WIDAR 3.0 dataset it achieved 99.27% accuracy for a group of 6 persons.

As for RSSI, an indoor localization system has been developed. Support Vector Machine(SVM) and k-Nearest Neighbors(kNN) classification methods have been utilized and the results for SVM were as follows: Gaussian Radial Basis Function(RBF) SVM test accuracy is 97.811% and poly SVM test accuracy is 96.801%. For kNN, the accuracy results were as follows: 99.66% for training and 99.306% for testing.

7.2 Technical Future Vision

WiFi sensing shows promising results as we show and due to its low cost so we are going to go deeper with tasks that we have dealt with on the other hand we are going to add more systems that interact with healthcare and agriculture like respiration analysis, sleeping monitoring, fall detection, and moisture monitoring.

1. Intrusion Task:

- In regards to dataset: More data samples will be collected using more volunteers as it has shown better results with a huge amount of data that is required by the deep learning model to achieve generalization.
- In regards to algorithms: In the future unsupervised learning algorithms will be used to skip the stage of data labeling and make it easy for the normal user to use our system.
- In regards to system functions: the intrusion system will be tuned until achieving a stable, scalable, and reliable system is achieved.

2. Localization Task:

- In regards to dataset : More data samples will be collected as it has shown better results with a huge amount of data that is required by the deep learning model to achieve generalization. We are going to use CSI data instead of RSSI in some environments for passive localization

7.2 Technical Future Vision

- In regards to algorithms: In the future variational autoencoder will be used to match each grid cell with the dataset.
- In regards to system functions: A localization function will be added to the system until a multitasking, stable and reliable system is achieved.

3. Gait and Joint Task:

- In regards to dataset: More data samples will be collected using more volunteers as it has shown better results with WIDAR 3.0 dataset due to the huge amount of data that is required by the deep learning model to achieve generalization.
- In regards to algorithms: In the future Siamese network and a variational autoencoder will be used, then latent space will be used as an output with a classifier and more advanced algorithms will be utilized like, transformers.
- In regards to system functions: A localization function will be added to the system until a multitasking, stable and reliable system is achieved.

4. Respiration Analysis

- covid -19 pandemic shows the importance of contactless technologies especially in the healthcare system so we will focus on respiration analysis with CSI.
- In regards to dataset: we are going to find volunteers to participate in our next experiments for contactless respiration analysis using WiFi sensing.
- In regards to algorithms: we are going to build custom learning algorithms to achieve our goal.
- In regards to system functions: the system must be stable and reliable.

REFERENCES

- [1] M. Amjadi, K.-U. Kyung, I. Park, and M. Sitti, “Stretchable, skin mountable, and wearable strain sensors and their potential applications: A review,” *Adv. Funct. Mater.*, vol. 26, no. 11, pp. 1678–1698, Mar. 2016.
- [2] S.-R. Ke, H. L. U. Thuc, Y.-J. Lee, J.-N. Hwang, J.-H. Yoo, and K.-H. Choi, “A review on video-based human activity recognition,” *Computers*, vol. 2, no. 2, pp. 88–131, 2013. [Online]. Available: <https://www.mdpi.com/2073-431X/2/2/88>
- [3] A. Sciarrone, C. Fiandrino, I. Bisio, F. Lavagetto, D. Kliazovich, and P. Bouvry, “Smart probabilistic fingerprinting for indoor localization over fog computing platforms,” in Proc. 5th IEEE Int. Conf. Cloud Netw. (Cloudnet), Oct. 2016, pp. 39–44.
- [4] Z. Zhou, C. S. Wu, Z. Yang, and Y. H. Liu, “Sensorless sensing with wifi,” *Tsinghua Science and Technology*, vol. 20, no. 1, pp. 1–6, Feb. 2015.
- [5] A. Vlavianos, L. K. Law, I. Broustis, S. V. Krishnamurthy, and M. Faloutsos, “Assessing link quality in ieee 802.11 wireless networks: Which is the right metric?” in 2008 IEEE 19th International Symposium on Personal, Indoor and Mobile Radio Communications, Sep. 2008, pp. 1–6.
- [6] Z. Yang, Z. Zhou, and Y. Liu, “From rssi to csi: indoor localization via channel response,” *ACM Computing Survey*, vol. 46, no. 2, pp. 25:1– 25:32, Dec. 2013.
- [7] X. Yang, “IEEE 802.11 n: enhancements for higher throughput in wireless LANs,” *IEEE Wireless Communications*, vol. 12, no. 6, pp. 82–91, 2005.
- [8] Malathi P, Vanathi PT. (2008). Orthogonal Frequency Division Multiplexing (OFDM) for wireless Local Area Network (WLAN) systems. *Adv. Model. Anal. B* 51(1-2): 1–16.

REFERENCES

- [9] D. Halperin, W. Hu, A. Sheth, and D. Wetherall, “Tool release: Gathering 802.11n traces with channel state information,” ACM SIGCOMM CCR, vol. 41, no. 1, p. 53, Jan. 2011.
- [10] W. Wang, A. Liu, M. Shahzad, K. Ling, and S. Lu, “Understanding and modelling of WiFi signal based human activity recognition,” in Proc. of the 21st Annual Int. Conf. on Mobile Computing and Networking. ACM, 2015, pp. 65–76.
- [11] S. Sen, B. Radunovic, R. R. Choudhury, and T. Minka, “You are facing the mona lisa: spot localization using phy layer information,” in Proc. of the 10th Int. Conf. on Mobile systems, applications, and services. ACM, 2012, pp. 183–196.
- [12] Wang Y., Liu J., Chen Y., Gruteser M., Yang J., Liu H. E-eyes: Device-Free location-oriented activity identification using fine-grained wifi signatures; Proceedings of the 20th ACM Annual International Conference on Mobile Computing and Networking; Maui, HI, USA. 7–11 September 2014; pp. 617–628.
- [13] Fadel Adib and Dina Katabi. 2013. See Through Walls with WiFi!. In Proceedings of the ACM SIGCOMM 2013 Conference on SIGCOMM (SIGCOMM ’13). 75–86.
- [14] Kun Qian, Chenshu Wu, Zheng Yang, Yunhao Liu, and Zimu Zhou. 2014. PADS: Passive Detection of Moving Targets with Dynamic Speed Using PHY Layer Information. In 2014 20th IEEE International Conference on Parallel and Distributed Systems (ICPADS). 1–8.
- [15] Chenshu Wu, Zheng Yang, Zimu Zhou, Xuefeng Liu, Yunhao Liu, and Jiannong Cao. 2015. Non-Invasive Detection of Moving and Stationary Human With WiFi. IEEE Journal on Selected Areas in Communications 33, 11 (Nov 2015), 2329–2342.
- [16] Rui Zhou, Xiang Lu, Pengbiao Zhao, and Jiesong Chen. 2017. Device-free Presence Detection and Localization With SVM and CSI Fingerprinting. IEEE Sensors Journal 17, 23 (Dec 2017), 7990–7999.
- [17] Daqing Zhang, Hao Wang, Yasha Wang, and Junyi Ma. 2015. Anti-fall: A Non-intrusive and Real-Time Fall Detector Leveraging CSI from Commodity WiFi Devices. In Inclusive Smart Cities and e-Health. Springer International Publishing, 181–193.

REFERENCES

- [18] Hao Wang, Daqing Zhang, Yasha Wang, Junyi Ma, Yuxiang Wang, and Shengjie Li. 2017. RT-Fall: A Real-Time and Contactless Fall Detection System with Commodity WiFi Devices. *IEEE Transactions on Mobile Computing* 16, 2 (Feb. 2017), 511–526.
- [19] Chunmei Han, Kaishun Wu, Yuxi Wang, and Lionel M. Ni. 2014. WiFall: Device-free Fall Detection by Wireless Networks. In 2014 IEEE Conference on Computer Communications (INFOCOM). 271–279.
- [20] Jialin Liu, Lei Wang, Linlin Guo, Jian Fang, Bingxian Lu, and Wei Zhou. 2017. A Research on CSI-based Human Motion Detection in Complex Scenarios. In 2017 IEEE 19th International Conference on e-Health Networking, Applications and Services (Healthcom). 1–6. <https://doi.org/10.1109/HealthCom.2017.8210800>
- [21] Yu Gu, Jinhai Zhan, Yusheng Ji, Jie Li, Fuji Ren, and Shangbing Gao. 2017. MoSense: An RF-based Motion Detection System via Off-the-Shelf WiFi Devices. *IEEE Internet of Things Journal* 4, 6 (Dec 2017), 2326–2341. <https://doi.org/10.1109/JIOT.2017.2754578>
- [22] Sheheryar Arshad, Chunhai Feng, Yonghe Liu, Yupeng Hu, Ruiyun Yu, Siwang Zhou, and Heng Li. 2017. Wi-Chase: A WiFi based Human Activity Recognition System for Sensorless Environments. In 2017 IEEE 18th International Symposium on A World of Wireless, Mobile and Multimedia Networks (WoWMoM). 1–6. <https://doi.org/10.1109/WoWMoM.2017.7974315>
- [23] Biyi Fang, Nicholas D. Lane, Mi Zhang, and Fahim Kawsar. 2016. HeadScan: A Wearable System for Radio-based Sensing of Head and Mouth-Related Activities. In 2016 15th ACM/IEEE International Conference on Information Processing in Sensor Networks (IPSN). 1–12. <https://doi.org/10.1109/IPSN.2016.7460677>
- [24] Qinhua Gao, Jie Wang, Xiaorui Ma, Xueyan Feng, and Hongyu Wang. 2017. CSI-based Device-free Wireless Localization and Activity Recognition Using Radio Image Features. *IEEE Transactions on Vehicular Technology* 66, 11 (Nov 2017), 10346–10356. <https://doi.org/10.1109/TVT.2017.2737553>
- [25] Wei Wang, Alex X. Liu, Muhammad Shahzad, Kang Ling, and Sanglu Lu. 2017. Device-free Human Activity Recognition Using Commercial WiFi Devices.

REFERENCES

- IEEE Journal on Selected Areas in Communications 35, 5 (May 2017), 1118–1131.
<https://doi.org/10.1109/JSAC.2017.2679658>
- [26] Fu Xiao, Jing Chen, Xiao Hui Xie, Linqing Gui, Juan Li Sun, and Wang Ruchuan. 2018. SEARE: A System for Exercise Activity Recognition and Quality Evaluation Based on Green Sensing. IEEE Transactions on Emerging Topics in Computing (2018). <https://doi.org/10.1109/TETC.2018.2790080>
- [27] Heba Abdelnasser, Moustafa Youssef, and Khaled A. Harras. 2015. WiGest: A Ubiquitous WiFi-based Gesture Recognition System. In 2015 IEEE Conference on Computer Communications (INFOCOM). 1472–1480. <https://doi.org/10.1109/INFOCOM.2015.7218525>
- [28] Kamran Ali, Alex X. Liu, Wei Wang, and Muhammad Shahzad. 2017. Recognizing Keystrokes Using WiFi Devices. IEEE Journal on Selected Areas in Communications 35, 5 (May 2017), 1175–1190. <https://doi.org/10.1109/JSAC.2017.2680998>
- [29] Yongsen Ma, Gang Zhou, Shuangquan Wang, Hongyang Zhao, and Woosub Jung. 2018. SignFi: Sign Language Recognition Using WiFi. Proc. ACM Interact. Mob. Wearable Ubiquitous Technol. 2, 1, Article 23 (March 2018), 21 pages. <https://doi.org/10.1145/3191755>
- [30] Hongbo Liu, Yan Wang, Jian Liu, Jie Yang, Yingying Chen, and H. Vincent Poor. 2018. Authenticating Users Through Fine-Grained Channel Information. IEEE Transactions on Mobile Computing 17, 2 (Feb 2018), 251–264. <https://doi.org/10.1109/TMC.2017.2718540>
- [31] Wei Wang, Yingjie Chen, and Qian Zhang. 2016. Privacy-Preserving Location Authentication in Wi-Fi Networks Using Fine-Grained Physical Layer Signatures. IEEE Transactions on Wireless Communications 15, 2 (Feb 2016), 1218–1225. <https://doi.org/10.1109/TWC.2015.2487453>
- [32] Wei Wang, Alex X. Liu, and Muhammad Shahzad. 2016. Gait Recognition Using WiFi Signals. In Proceedings of the 2016 ACM International Joint Conference on Pervasive and Ubiquitous Computing (UbiComp '16). 363–373. <https://doi.org/10.1145/2971648.2971670>

REFERENCES

- [33] Ju Wang, Hongbo Jiang, Jie Xiong, Kyle Jamieson, Xiaojiang Chen, Dingyi Fang, and Binbin Xie. 2016. LiFS: Low Human-effort, Device-free Localization with Fine-grained Subcarrier Information. In Proceedings of the 22Nd Annual International Conference on Mobile Computing and Networking (MobiCom '16). ACM, 243–256. <https://doi.org/10.1145/2973750.2973776>
- [34] Rui Zhou, Xiang Lu, Pengbiao Zhao, and Jiesong Chen. 2017. Device-free Presence Detection and Localization With SVM and CSI Fingerprinting. *IEEE Sensors Journal* 17, 23 (Dec 2017), 7990–7999. <https://doi.org/10.1109/JSEN.2017.2762428>
- [35] Heba Abdelnasser, Khaled A. Harras, and Moustafa Youssef. 2015. UbiBreathe: A Ubiquitous non-Invasive WiFi-based Breathing Estimator. In Proceedings of the 16th ACM International Symposium on Mobile Ad Hoc Networking and Computing (MobiHoc '15). 277–286. <https://doi.org/10.1145/2746285.2755969>
- [36] Xuefeng Liu, Jiannong Cao, Shaojie Tang, Jiaqi Wen, and Peng Guo. 2016. Contactless Respiration Monitoring Via Off-the-Shelf WiFi Devices. *IEEE Transactions on Mobile Computing* 15, 10 (Oct 2016), 2466–2479. <https://doi.org/10.1109/TMC.2015.2504935>
- [37] Pei Wang, Bin Guo, Tong Xin, Zhu Wang, and Zhiwen Yu. 2017. TinySense: Multi-User Respiration Detection Using Wi-Fi CSI Signals. In 2017 IEEE 19th International Conference on e-Health Networking, Applications and Services (Healthcom). 1–6. <https://doi.org/10.1109/HealthCom.2017.8210837>
- [38] Fusang Zhang, Daqing Zhang, Jie Xiong, Hao Wang, Kai Niu, Beihong Jin, and Yuxiang Wang. 2018. From Fresnel Diffraction Model to Fine-grained Human Respiration Sensing with Commodity Wi-Fi Devices. *Proc. ACM Interact. Mob. Wearable Ubiquitous Technol.* 2, 1, Article 53 (March 2018), 23 pages. <https://doi.org/10.1145/3191785>
- [39] L. Takayama, C. Pantofaru, D. Robson, B. Soto, and M. Barry, “Making technology homey: Finding sources of satisfaction and meaning in home automation,” in Proceedings of the 2012 ACM Conference on Ubiquitous Computing, ser. UbiComp '12. New York, NY, USA: Association for Computing Machinery, 2012, p. 511–520. [Online]. Available: <https://doi.org/10.1145/2370216.2370292>

REFERENCES

- [40] W. Mao, J. He, and L. Qiu, “Cat: High-precision acoustic motion tracking.” [Online]. Available: https://www.cs.utexas.edu/~jianhe/cat_mobicom.pdf
- [41] W. Wang, A. X. Liu, and K. Sun, “Device-free gesture tracking using acoustic signals,” in Proceedings of the 22nd Annual International Conference on Mobile Computing and Networking, ser. MobiCom ’16. New York, NY, USA: Association for Computing Machinery, 2016, p. 82–94. [Online]. Available: <https://doi.org/10.1145/2973750.2973764>
- [42] J. Han and B. Bhanu, “Human activity recognition in thermal infrared imagery,” in 2005 IEEE Computer Society Conference on Computer Vision and Pattern Recognition (CVPR’05) - Workshops, 2005, pp. 17–17.
- [43] O. Kaltiokallio, M. Bocca, and N. Patwari, “Enhancing the accuracy of radio tomographic imaging using channel diversity,” in 2012 IEEE 9th International Conference on Mobile Ad-Hoc and Sensor Systems (MASS 2012), 2012, pp. 254–262.
- [44] L. Liu, W. Zhang, C. Deng, S. Yin, and S. Wei, “Briguard: a lightweight indoor intrusion detection system based on infrared light spot displacement,” IET Science, Measurement Technology, vol. 9, no. 3, pp. 306–314, 2015.
- [45] J. Xiao, K. Wu, Y. Yi, L. Wang, and L. M. Ni, “Fimd: Fine-grained devicefree motion detection,” in 2012 IEEE 18th International Conference on Parallel and Distributed Systems, 2012, pp. 229–235.
- [46] C. Wu, Z. Yang, Z. Zhou, X. Liu, Y. Liu, and J. Cao, “Non-invasive detection of moving and stationary human with wifi,” IEEE Journal on Selected Areas in Communications, vol. 33, no. 11, pp. 2329–2342, 2015.
- [47] Z. Zhou, Z. Yang, C. Wu, L. Shangguan, and Y. Liu, “Omnidirectional coverage for device-free passive human detection,” IEEE Transactions on Parallel and Distributed Systems, vol. 25, no. 7, pp. 1819–1829, 2014.
- [48] S. Li, Z. Liu, Y. Zhang, X. Niu, L. Wang, and D. Zhang, “A real-time and robust intrusion detection system with commodity wi-fi,” ser. UbiComp/ISWC ’19 Adjunct. New York, NY, USA: Association for Computing Machinery, 2019, p. 316–319. [Online]. Available: <https://doi.org/10.1145/3341162.3343789>

REFERENCES

- [49] Y. Lin, Y. Gao, B. Li, and W. Dong, “Revisiting indoor intrusion detection with wifi signals: Do not panic over a pet!” IEEE Internet of Things Journal, vol. 7, no. 10, pp. 10 437–10 449, 2020.
- [50] X. Yang, S. Wu, M. Zhou, L. Xie, J. Wang, and W. He, “Indoor throughthe- wall passive human target detection with wifi,” in 2019 IEEE Globecom Workshops (GC Wkshps), 2019, pp. 1–6.
- [51] E. O. Brigham and R. E. Morrow, ”The fast Fourier transform,” Dec. 1967.
- [52] James W. Cooley, Peter A. W. Lewis and Peter D. Welch, ” The Fast Fourier Transform and Its Applications,” March 1969.
- [53] M.A. Hearst, S.T. Dumais, E. Osuna, J. Platt and B. Scholkopf, ” Support vector machines,” July-Aug. 1998.
- [54] J. Laaksonen and E. Oja, ”Classification with learning k-nearest neighbors,” 06 August 2002
- [55] I. T. Jolliffe, Principal Component Analysis, 2nd ed. New York, NY, USA: Springer, 2002.
- [56] Anil K. Jain, Nalini K. Ratha, Sridhar Lakshmanan, Object detection using gabor filters, Pattern Recognition, Volume 30, Issue 2, 1997, Pages 295-309, ISSN 0031-3203, [https://doi.org/10.1016/S0031-3203\(96\)00068-4](https://doi.org/10.1016/S0031-3203(96)00068-4).
- [57] Martin Ester, Hans-Peter Kriegel, Jörg Sander and Xiaowei Xu, ”A density-based algorithm for discovering clusters in large spatial databases with noise”.August 1996
- [58] M. Youssef, M. Mah, and A. Agrawala, “Challenges: Device-free passive localization for wireless environments.” New York, NY, USA: Association for Computing Machinery, 2007. [Online]. Available: <https://doi.org/10.1145/1287853.1287880>
- [59] L. Wei, R. Q. Hu, Y. Qian, and G. Wu, “Enable device-to-device communications underlaying cellular networks: challenges and research aspects,” IEEE Communications Magazine, vol. 52, no. 6, pp. 90–96, 2014.

REFERENCES

- [60] M. Ahmad, A. M. Khan, J. A. Brown, S. Protasov, and A. M. Khattak, “Gait fingerprinting-based user identification on smartphones,” in 2016 International Joint Conference on Neural Networks (IJCNN), 2016, pp. 3060–3067.
- [61] F. Horst, S. Lapuschkin, W. Samek, K.-R. Müller, and W. I. Schöllhorn, “Explaining the unique nature of individual gait patterns with deep learning,” *Scientific Reports*, vol. 9, no. 1, 2019.
- [62] J. Chen, “Gait correlation analysis based human identification,” *The Scientific World Journal*, vol. 2014, pp. 1–8, 2014.
- [63] J. E. Cutting and L. T. Kozlowski, “Recognizing friends by their walk: Gait perception without familiarity cues,” *Bulletin of the Psychonomic Society*, vol. 9, no. 5, pp. 353–356, 1977.
- [64] M. P. MURRAY, A. B. DROUGHT, and R. C. KORY, “Walking patterns of normal men,” *The Journal of Bone Joint Surgery*, vol. 46, no. 2, pp. 335–360, 1964.
- [65] D. Gafurov, E. Snekkenes, and P. Bours, “Spoof attacks on gait authentication system,” *IEEE Transactions on Information Forensics and Security*, vol. 2, no. 3, pp. 491–502, 2007.
- [66] Lecture Notes in Computer Science, 2011.
- [67] G. Johansson, “Visual perception of biological motion and a model for its analysis,” *Perception Psychophysics*, vol. 14, no. 2, pp. 201–211, 1973.
- [68] J. E. Cutting, D. R. Proffitt, and L. T. Kozlowski, “A biomechanical invariant for gait perception.” *Journal of Experimental Psychology: Human Perception and Performance*, vol. 4, no. 3, pp. 357–372, 1978.
- [69] N. Boulgouris, D. Hatzinakos, and K. Plataniotis, “Gait recognition: a challenging signal processing technology for biometric identification,” *IEEE Signal Processing Magazine*, vol. 22, no. 6, pp. 78–90, 2005.
- [70] L. Lee and W. Grimson, “Gait analysis for recognition and classification,” in *Proceedings of Fifth IEEE International Conference on Automatic Face Gesture Recognition*, 2002, pp. 155–162.

REFERENCES

- [71] T. H. Lam, K. Cheung, and J. N. Liu, “Gait flow image: A silhouette-based gait representation for human identification,” *Pattern Recognition*, vol. 44, no. 4, pp. 973–987, 2011.
- [72] M. S. Nixon, J. N. Carter, D. Cunado, P. S. Huang, and S. V. Stevenage, “Automatic gait recognition,” *Biometrics*, pp. 231–249.
- [73] R. J. Orr and G. D. Abowd, “The smart floor: A mechanism for natural user identification and tracking,” in *CHI ’00 Extended Abstracts on Human Factors in Computing Systems*, ser. CHI EA ’00. New York, NY, USA: Association for Computing Machinery, 2000, p. 275–276. [Online]. Available: <https://doi.org/10.1145/633292.633453>
- [74] S. Sprager and D. Zazula, “A cumulant-based method for gait identification using accelerometer data with principal component analysis and support vector machine,” *WSEAS Trans. Sig. Proc.*, vol. 5, no. 11, p. 369–378, Nov. 2009.
- [75] A. Primo, V. V. Phoha, R. Kumar, and A. Serwadda, “Context-aware active authentication using smartphone accelerometer measurements,” in *2014 IEEE Conference on Computer Vision and Pattern Recognition Workshops*, 2014, pp. 98–105.
- [76] F. Zhang, K. Niu, J. Xiong, B. Jin, T. Gu, Y. Jiang, and D. Zhang, “Towards a diffraction-based sensing approach on human activity recognition,” *Proc. ACM Interact. Mob. Wearable Ubiquitous Technol.*, vol. 3, no. 1, Mar. 2019. [Online]. Available: <https://doi.org/10.1145/3314420>
- [77] Y. Ma, G. Zhou, S. Wang, H. Zhao, and W. Jung, “Signfi: Sign language recognition using wifi,” *Proc. ACM Interact. Mob. Wearable Ubiquitous Technol.*, vol. 2, no. 1, Mar. 2018. [Online]. Available: <https://doi.org/10.1145/3191755>
- [78] G. Wang, Y. Zou, Z. Zhou, K. Wu, and L. M. Ni, “We can hear you with wifi!” *IEEE Transactions on Mobile Computing*, vol. 15, no. 11, pp. 2907– 2920, 2016.
- [79] Z. Fu, J. Xu, Z. Zhu, A. X. Liu, and X. Sun, “Writing in the air with wifi signals for virtual reality devices,” *IEEE Transactions on Mobile Computing*, vol. 18, no. 2, pp. 473–484, 2019.
- [80] W. Wang, A. X. Liu, and M. Shahzad, “Gait recognition using wifi signals,” in *Proceedings of the 2016 ACM International Joint Conference on Pervasive and Ubiquitous*

REFERENCES

- Computing, ser. UbiComp '16. New York, NY, USA: Association for Computing Machinery, 2016, p. 363–373. [Online]. Available: <https://doi.org/10.1145/2971648.2971670>
- [81] Y. Zeng, P. H. Pathak, and P. Mohapatra, “Wiwho: Wifi-based person identification in smart spaces,” ser. IPSN ’16. IEEE Press, 2016.
- [82] Y. Xu, W. Yang, J. Wang, X. Zhou, H. Li, and L. Huang, “Wistep: Device-free step counting with wifi signals,” Proc. ACM Interact. Mob. Wearable Ubiquitous Technol., vol. 1, no. 4, Jan. 2018. [Online]. Available: <https://doi.org/10.1145/3161415>
- [83] J. Zhang, B. Wei, W. Hu, and S. S. Kanhere, “Wifi-id: Human identification using wifi signal,” in 2016 International Conference on Distributed Computing in Sensor Systems (DCOSS), 2016, pp. 75–82.
- [84] J. Wright, A. Y. Yang, A. Ganesh, S. S. Sastry, and Y. Ma, “Robust face recognition via sparse representation,” IEEE Transactions on Pattern Analysis and Machine Intelligence, vol. 31, no. 2, pp. 210–227, 2009.
- [85] Y. Chen, W. Dong, Y. Gao, X. Liu, and T. Gu, “Rapid: a multimodal and device-free approach using noise estimation for robust person identification,” ACM Proceedings on Interactive, Mobile, Wearable and Ubiquitous Technologies, vol. 1, no. 3, sep 2017.
- [86] D. Halperin, W. Hu, A. Sheth, and D. Wetherall, “Tool release: Gathering 802.11n traces with channel state information,” ACM SIGCOMM CCR, vol. 41, no. 1, p. 53, Jan. 2011.
- [87] V. Bazarevsky, Y. Kartynnik, A. Vakunov, K. Raveendran, and M. Grundmann, “Blaze-face: Sub-millisecond neural face detection on mobile gpus,” 2019.
- [88] M. Sandler, A. Howard, M. Zhu, A. Zhmoginov, and L.-C. Chen, “Mobilenetv2: Inverted residuals and linear bottlenecks,” 2019.
- [89] F. Chollet, “Xception: Deep learning with depthwise separable convolutions,” in 2017 IEEE Conference on Computer Vision and Pattern Recognition (CVPR), 2017, pp. 1800–1807.
- [90] K. He, X. Zhang, S. Ren, and J. Sun, “Deep residual learning for image recognition,” 2015.

REFERENCES

- [91] D. P. Kingma and J. Ba, “Adam: A method for stochastic optimization,” arXiv preprint arXiv:1412.6980, 2014.
- [92] Z. Y. Y. Z. G. Z. Y. Zheng, “Widar 3.0: Wifi-based activity recognition dataset,” 2020. [Online]. Available: <https://dx.doi.org/10.21227/7znf-qp86>
- [93] Y. Zhang, Y. Zheng, G. Zhang, K. Qian, C. Qian, and Z. Yang, “Gaitid: Robust wi-fi based gait recognition.” [Online]. Available: http://tns.thss.tsinghua.edu.cn/widar3.0/data/WASA20_GaitID_paper.pdf
- [94] ——, “Gaitid: Robust wi-fi based gait recognition,” in Wireless Algorithms, Systems, and Applications, D. Yu, F. Dressler, and J. Yu, Eds. Cham: Springer International Publishing, 2020, pp. 730–742.
- [95] J. Ding, Y. Wang, and X. Fu, “Wihi: Wifi based human identity identification using deep learning,” IEEE Access, vol. 8, pp. 129 246–129 262, 2020.
- [96] J. Lv, W. Yang, D. Man, X. Du, M. Yu, and M. Guizani, “Wii: Devicefree passive identity identification via wifi signals,” in GLOBECOM 2017 - 2017 IEEE Global Communications Conference, 2017, pp. 1–6.
- [97] Y. Zeng, P. H. Pathak, and P. Mohapatra, “Wiwho: Wifi-based person identification in smart spaces,” in 2016 15th ACM/IEEE International Conference on Information Processing in Sensor Networks (IPSN), 2016, pp. 1–12.
- [98] L. Zhang, C. Wang, M. Ma, and D. Zhang, “Widigr: Direction-independent gait recognition system using commercial wi-fi devices,” IEEE Internet of Things Journal, vol. 7, no. 2, pp. 1178–1191, 2020.
- [99] T. Nguyen, Y. Jeong, D. Trinh and H. Shin, ”Location-aware visual radios”, IEEE Wireless Commun., vol. 21, no. 4, pp. 28-36, Aug. 2014.
- [100] A. Rai, K. K. Chintalapudi, V. N. Padmanabhan and R. Sen, ”Zee: Zero-effort crowdsourcing for indoor localization”, Proc. 18th Annu. Int. Conf. Mobile Comput. Netw., pp. 293-304, 2012.

REFERENCES

- [101] Q. Jiang, Y. Ma, K. Liu and Z. Dou, "A probabilistic radio map construction scheme for crowdsourcing-based fingerprinting localization", IEEE Sensors J., vol. 16, no. 10, pp. 3764-3774, May 2016.
- [102] J. G. Park et al., "Growing an organic indoor location system", Proc. ACM 8th Int. Conf. Mobile Syst. Appl. Services, pp. 271-284, Jun. 2010.
- [103] P. Mirowski, K. H. Tin, Y. Saehoon and M. Macdonald, "SignalSLAM: Simultaneous localization and mapping with mixed WiFi Bluetooth LTE and magnetic signals", Proc. IPIN, pp. 1-10, Oct. 2013.
- [104] C. Wu, Z. Yang and Y. Liu, "Smartphones based crowdsourcing for indoor localization", IEEE Trans. Mobile Comput., vol. 14, no. 2, pp. 444-457, Feb. 2015.
- [105] S. N. He, B. Ji and S. H. Chan, "Chameleon: Survey-free updating of a fingerprint database for indoor localization", IEEE Pervasive Comput., vol. 15, no. 4, pp. 66-75, Oct./Dec. 2016.
- [106] B. Wang, Q. Chen, L. T. Yang and H.-C. Chao, "Indoor smartphone localization via fingerprint crowdsourcing: Challenges and approaches", IEEE Wireless Commun., vol. 23, no. 3, pp. 82-89, Jun.
- [107] Y. Zhuang, Z. Syed, Y. Li and N. El-Sheimy, "Evaluation of two WiFi positioning systems based on autonomous crowdsourcing of handheld devices for indoor navigation", IEEE Trans. Mobile Comput., vol. 15, no. 8, pp. 1982-1995, Aug. 2016.
- [108] Á. Utasi and C. Benedek, "A Bayesian approach on people localization in multicamera systems", IEEE Trans. Circuits Syst. Video Technol., vol. 23, no. 1, pp. 105-115, Jan. 2013.
- [109] L. Liu, X. Zhang and H. D. Ma, "Localization-oriented coverage in wireless camera sensor networks", IEEE Trans. Wireless Commun., vol. 10, no. 2, pp. 484-494, Feb. 2011.
- [110] Y. Liu, Q. Wang, J. Liu, J. Chen and T. Wark, "An efficient and effective localization method for networked disjoint top-view cameras", IEEE Trans. Instrum. Meas., vol. 62, no. 9, pp. 2526-2537, Sep. 2013.

REFERENCES

- [111] R. Pflugfelder and H. Bischof, "Localization and trajectory reconstruction in surveillance cameras with nonoverlapping views", *IEEE Trans. Pattern Anal. Mach. Intell.*, vol. 32, no. 4, pp. 709-721, Apr. 2010.
- [112] Y. S. Lin, K. H. Lo, H. T. Chen and J. H. Chuang, "Vanishing point-based image transforms for enhancement of probabilistic occupancy map-based people localization", *IEEE Trans. Image Process.*, vol. 23, no. 12, pp. 5586-5598, Dec. 2014.
- [113] D. Macagnano, G. Destino and G. Abreu, "Localization with heterogeneous information", *Proc. IEEE WF-IOT*, pp. 124-129, Mar. 2014.
- [114] B. Denis et al., "Cooperative and heterogeneous indoor localization experiments", *Proc. IEEE ICC*, pp. 6-10, Jun. 2013.
- [115] H. B. Liu, J. Yang, S. Sidhom, Y. Wang, Y. Y. Chen and F. Ye, "Accurate WiFi based localization for smartphone using peer assistance", *IEEE Trans. Mobile Comput.*, vol. 13, no. 10, pp. 2199-2214, Oct. 2014.
- [116] Z. H. Chen, Q. C. Zhu and Y. C. Soh, "Smartphone inertial sensor-based indoor localization and tracking with iBeacon corrections", *IEEE Trans. Ind. Informat.*, vol. 12, no. 4, pp. 1540-1549, Aug. 2016.
- [117] Y. Chen, D. Lymberopoulos, J. Liu and B. Priyantha, "Indoor localization using FM signals", *IEEE Trans. Mobile Comput.*, vol. 12, no. 8, pp. 1502-1517, Aug. 2013.
- [118] M. Youssef, M. Mah, and A. Agrawala, "Challenges: device-free passive localization for wireless environments," in *Proceedings of ACM MobiCom*, 2007, pp. 222–229.
- [119] N. Patwari and J. Wilson, "Rf sensor networks for device-free localization: Measurements, models, and algorithms," *Proceedings of the IEEE*, vol. 98, no. 11, pp. 1961–1973, 2010.
- [120] I. W. Selesnick and C. S. Burrus, "Generalized digital Butterworth filter design," in *IEEE Transactions on Signal Processing*, vol. 46, no. 6, pp. 1688-1694, June 1998, doi: 10.1109/78.678493.

REFERENCES

- [121] Daniel Halperin et al. ‘Tool Release: Gathering 802.11n Traces with Channel State Information’. In: ACM SIGCOMM CCR 41.1 (2011), p. 53. url: http://www.halper.in/pubs/halperin_csitool.pdf.
- [122] Yaxiong Xie, Zhenjiang Li and Mo Li. ‘Precise power delay profiling with commodity Wi-Fi’. In: IEEE Transactions on Mobile Computing (2018).
- [123] ThinkWiki. problem with unauthorized MiniPCI network card. url:https://www.thinkwiki.org/wiki/Problem_with_unauthorized_MiniPCI_network_card.
- [124] Ubuntu.Ubuntu Kernel Support and Schedules. url:<https://wiki.ubuntu.com/Kernel/Support>
- [125] ”Index of /releases/14.04.3”, Old-releases.ubuntu.com, 2021. [Online]. Available: <http://old-releases.ubuntu.com/releases/14.04.3/>.
- [126] ”Linux 802.11n CSI Tool — Installation Instructions”, Dhalperi.github.io, 2021. [Online]. Available: <https://dhalperi.github.io/linux-80211n-csitool/installation.html>.